MASTER IN BIOCHEMISTRY AND MOLECULAR AND CELLULAR BIOLOGY

Involvement og MAGEA1 gene in tumorigensis
In vivo and in vitro models

WILLEMS , Estelle

Award date:
2014

Awarding institution:
University of Namur

UNIVERSITE DE NAMUR

Faculté des Sciences

INVOLVEMENT OF MAGEA1 GENE IN TUMORIGENESIS *IN VIVO* AND *IN VITRO* MODELS

Mémoire présenté pour l'obtention

du grade académique de master en biochimie et biologie moléculaire et cellulaire

Estelle Willems

Janvier 2013

UNIVERSITÉ DE NAMUR

Master 2 BBMC
January 2013
Lab of Genetics, URPHYM
Promoter: Olivier De Backer
Supervisor: Elise Srour

INVOLVEMENT OF MAGEA1 GENE IN TUMORIGENESIS: *IN VIVO* AND *IN VITRO* MODELS

WILLEMS Estelle

ABSTRACT

MAGEA1, a member of type I melanoma antigens genes (MAGE), is only expressed in male germ cells and in cancer cells of several histological types. Some evidences support the hypothesis that MAGEA genes are expressed to provide a survival advantage to tumor cells. First, type I MAGE genes are able to inhibit the activity and decrease the level of the tumor suppressor p53. Secondly, MAGEA gene expression is associated with tumor invasiveness, lymph node metastasis, poor prognosis and advanced clinical stage. Moreover, MAGEA1 expression is also associated with increased chemoresistance. The purpose of my work was to study the involvement of MAGEA1 in tumor development using *in vivo* and *in vitro* models.

The *in vivo* model involves the generation of transgenic mice expressing MAGEA1 ectopically in melanocytes. Expression of MAGEA1 transgene in mouse tissues was analyzed by quantitative RT-PCR. Preliminary results showed different levels of MAGEA1 transcripts in the skin of each mouse lineage, but not in the other examined tissues (testis, heart, liver and brain).

The second goal of my project was to study the oncogenic functions of MAGEA1 *in vitro*. Using cell survival assays, a mechanism of chemoresistance conferred by MAGEA1 was detected in two different cell models (MCF-10A and MCF-7 cells) after treatment with etoposide, 5-fluorouracil and docetaxel. Complementary survival tests on Hep3B cells, a p53-deficient cell model, did not reveal chemoresistance in presence of MAGEA1 except after docetaxel treatment, a drug reported to work independently of p53 pathway. Forced expression of MAGEA1 by transduction induced an overexpression of ABC transporters mRNA in MCF-10A cells but not in Hep3B cells. As these transporters are mediators of chemoresistance, the induction of ABC transporters by MAGEA1 could represent a new mechanism of the chemoresistance induced by MAGEA1. In parallel, cell migration assays indicated that MAGEA1 also conferred a migratory advantage to MCF-10A cells, but not to Hep3B.

ACKNOWLEDGEMENTS

Thanks to the professor Olivier De Backer for his welcome in the lab and for his sensible advices during my work

Thanks to Elise for her useful and precious assistance during all the period of my work

Thanks to Olivia, Domi, Coco, François, Christiane, Emilie, J-M, Gégé and all the lab of Genetics for their valuable help and their daily support

Thanks to the professors N. Caron, J-P Gillet, J-Y Matroule as well as V. Bourguignon for the time and attention dedicated for the reading of my report

Thanks to my father for his precious advices and support. Thanks to my mother and to Marie, Thibault, Adeline, Justine, Caro, etc for their precious encouragement and their moral support during this period

Thanks

SUMMARY

INTRODUCTION

I. CANCER TESTIS ANTIGENS

Since the 1980s, tumor specific antigens have raised the interest of many research teams in the field of anticancer immunotherapy (Fearon *et al*, 1988; Van Pel *et al*, 1992). Most of the clinical trials of tumor vaccination focus on melanoma, a cancer type characterized by numerous surface antigens (Chin *et al*, 2006).

Cancer testis antigens (CTA), a family of tumor specific antigens, are silenced in normal tissues except in cells of male germ-line. Interestingly, an ectopic expression of CTA has been identified in several histological tumor types, making them an attractive target for anticancer immunotherapy (Doyle *et al*, 2010; Gjerstorff *et al.*, 2008). CTA, derived from endogenous proteins, are presented on cell surface by molecules of the major histocompatibility complex (MHC) and recognized by cytotoxic T cells (van der Bruggen *et al*, 1991). The role of CTA is not yet defined, but some evidences support their implication in proliferation, differentiation and survival of germinal cells (Gjerstorff *et al*, 2008).

In 1991, van der Bruggen *et al* identified the gene coding for a CTA named MZ2-E (van der Bruggen *et al*, 1991). To this end, a cosmid library was prepared with the DNA of a melanoma cell line expressing MZ2-E and these cosmids were transfected in melanoma cells that do not express MZ2-E. Cell sensitivity to lymphocytes directed against MZ2 was tested, leading to the identification of MZ2-positive cells. This work allowed the identification of the gene which directs the expression of MZ2-E, now called MAGEA1 and presented by HLA-A1 molecules at the cell surface (Traversari *et al*, 1992).

II. MAGE GENE FAMILY

The melanoma antigen genes (MAGE) are divided in two main families: type I and type II MAGE genes, according to their expression pattern. Within these two families, MAGE genes are classified in different groups (MAGEA, MAGEB, etc) depending on their chromosomal localization and sequences similarity (De Plaen et al. 1994; Chomez *et al.*, 2001).

All MAGE proteins contain a well conserved domain of 165 to 170 amino acids, named Mage Homology Domain (MHD) (see Figure 1 and 2) (Chomez *et al.*, 2001). The amino acid sequence of this MHD is characterized by a global conservation rate of 46%. This conservation rate increases within MAGE subfamilies, with 75% between MAGED genes and 70% in the MAGEA family. This high conservation indicates an important role of the MHD that is not fully understood.

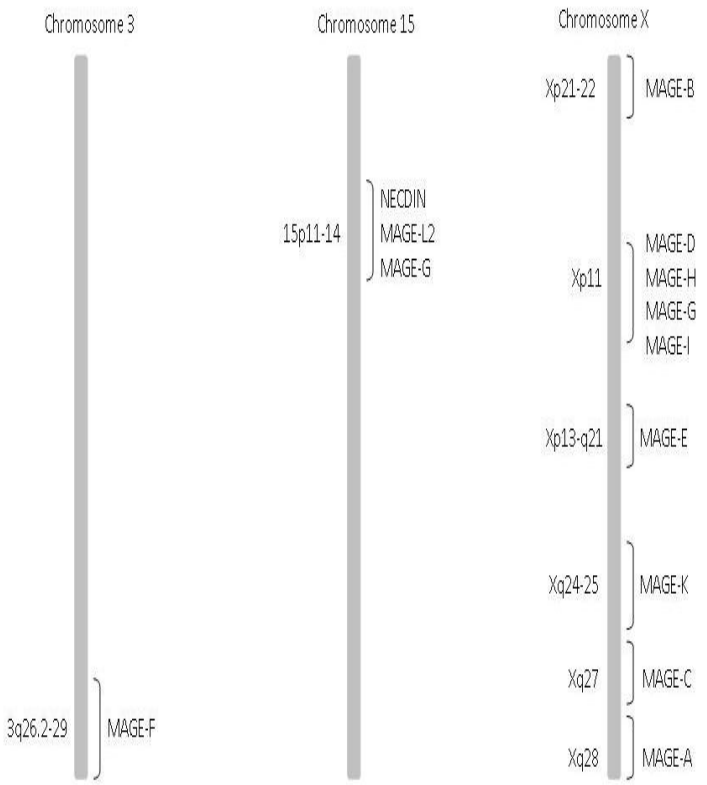

Figure 1: Chromosomal localization of human MAGE genes subfamilies

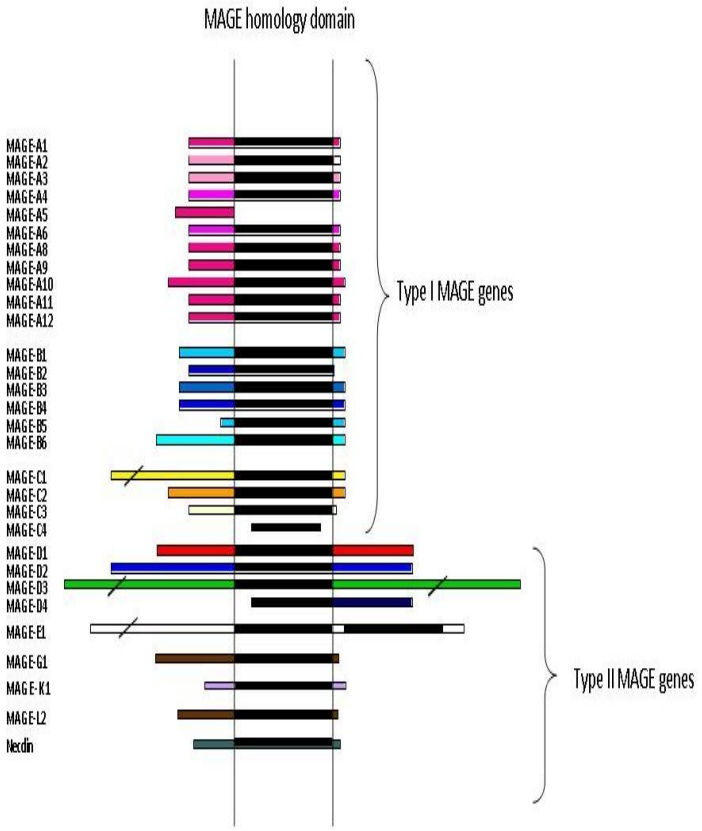

Figure 2: Illustration of the structural organization of MAGE proteins

Type I MAGE genes, present in clusters on the X chromosome, encode members of the CTA family that are exclusively expressed in male germ cells as well as at the surface of tumoral cells. Actually, some of the type I MAGE proteins are degraded through the proteasomal pathway in peptides. The MAGE peptides are then carried into the endoplasmic reticulum, associated with molecules of the class I HLA and presented to the cell membrane. Nowadays, more than thirty-five type I MAGE genes are described. Type I MAGE genes are divided in three sub-groups: 12 MAGEA genes are located in Xq28, 18 MAGEB in Xp21 and 7 MAGEC in Xq26-27 (Figure 1). At a structural level, type I MAGE genes are characterized by a large 3'-exon coding for the entire protein. The amino acid structure of type I MAGE proteins is limited to the MHD, surrounded by short C- and N-terminal sequences (Chomez *et al*, 2001).

Our work focuses on MAGEA1 gene that is expressed in 40% of melanomas, 17% of mammary carcinomas, 35% of non-small cell lung carcinomas and 21% of bladder carcinomas (De Smet *et al.*, 1995). MAGEA1 gene, spreading over 4,5 kilobases, contains three exons the first of which codes the entire protein.

The type II MAGE genes, present on the X chromosome and on autosomes, exhibit three main structural differences compared to type I MAGE genes. First, their coding sequence is spread on several exons. Then, type II MAGE proteins are structurally more complex, with longer N- and C-terminal extremities than most type I MAGE proteins. Finally, some type II MAGE genes have a duplicated MHD (namely, MAGEE1 and MAGEE2) (Barker & Salehi 2002; Doyle et al. 2010; Jung *et al*., 2005). Type II MAGE genes are expressed in various somatic cells at different developmental stages. Their role is not exactly determined, but some findings suggest an involvement in apoptosis, cell differentiation and, indirectly, in behaviour control (Dombret et al. 2012; Mouri et al. 2012; Wang et al. 2010). These last years, type II MAGE genes were being studied thoroughly in our lab. In 2010, Nguyen discovered that Maged1 mouse gene is required for proper skeletal myoblast differentiation and muscle healing (Nguyen *et al.*, 2010). Two years later, Dombret *et al* suggested that MAGE-D1 loss results in oxytocin production problems, deficits of social interactions, impaired sexual behavior and obesity (Dombret *et al*., 2012). A plausible hypothesis is that MAGE-D1 could play a role in autism or cause a neuro-developmental condition that is reminiscent of the Prader-Willi syndrome. Other type II MAGE genes are less characterized and further studies are needed to define their precise function.

III. TYPE I MAGE GENES

1) Expression pattern of type I MAGE genes

Type I MAGE genes are exclusively expressed in male germ cells and in cancer cells of several histological types such as brain, breast, liver, lung, ovary, prostate, skin, testis, thyroid and pancreatic cancers (Caballero *et al.*, 2010; Chomez *et al*., 1995; Doyle *et al.*, 2010; Takahashi *et al.*, 1995). The specific expression of MAGE proteins in tumoral tissues makes them an attractive target for immunotherapy (Sang *et al.*, 2010).

Regulation of transcription

Expression pattern of type I MAGE genes have intrigued the interest of several teams, such as that of De Smet *et al* who have studied the regulation of transcription (De Smet *et al.*, 1995). This team identified a family of transcription factors required for promoter activation, named Ets that are ubiquitously expressed in healthy somatic cells. The Ets binding domain present in the promoter of MAGEA1 is adjacent to a CpG island and can be silenced by methylation. Moreover, treatment with 5'aza-2'-deoxycytidine, a demethylating agent, was able to induce type I MAGE expression both in cancer and healthy cells (Weber *et al.*, 1994; De Smet *et al*, 1996; Jung *et al.*, 2004). These data are consistent with the correlation between the level of DNA methylation and the expression of MAGEA genes. Indeed, the percentage of genome methylation decreases to 29% in cancer cells positive for MAGEA1, for a level of 52% in cells not expressing MAGEA1 (De Smet *et al*, 1996; De Smet *et al*, 1999).

Actually, even if methylation is the predominant epigenetic regulation of MAGE genes expression, chromatin modulation influenced by histone acetyltransferases and deacetylases, also controls the expression of type I MAGE gene (Wischnewski *et al.*, 2006). These observations and others led to the conclusion that, in healthy cells, the expression of type I MAGE genes is prevented by DNA and histones methylation. It has been shown that other type I MAGE genes are regulated in the same way (De Smet *et al*., 1996; De Smet *et al*, 1999).

Afterwards, De Smet *et al* focused specifically on the epigenetic regulation of the MAGEA1 gene. They discovered that the hypo-methylation of the MAGEA1 promoter in cancerous cells relies on a transient process of de-methylation, followed by an inhibition of re-methylation by specific transcription factors (De Smet *et al*, 2004). This finding could explain why specific DNA sequences, such as MAGE promoters, stay un-methylated despite the activity of DNA methyltransferase (DNMT). Moreover, this hypothesis also gives an explanation for the characteristic pattern of methylation in tumor cells, corresponding to the coexistence of hypo-methylated and hyper-methylated regions (Ehrlich *et al*, 2002). The team tested his hypothesis by determining that the induction of a transient de-methylation phase, induced by inhibition of the DNMT1, was sufficient to convert a methylated MAGEA1 transgene into an un-methylated and active one (Loriot *et al*, 2006).

It is prominent to note that some CTA genes, including MAGE genes, are also expressed in trophoblast during embryogenesis. However, the developmental stage at which MAGE genes acquire DNA methylation marks was not yet determined. But in 2012, Loriot and his team demonstrated that the transcription of CTA genes increases up to the morula stage and then diminish drastically in blastocyst (Loriot *et al*, 2012). This observation suggests that CTA are programmed for repression in the blastocyst probably by *de novo* DNA methylation

It is not yet determined if the expression of type I MAGE genes is an epiphenomenon occurring after global hypomethylation in chaotic cancer cells, or if MAGE genes are expressed to provide a survival advantage to tumor cells.

Expression in mice

In 1995, De Backer and his team identified homologous genes of the human type I MAGE genes in mice (De Backer *et al*, 1995). Using a probe specific for the MAGEA1 human gene, they identified three homologous genes, initially named Smage-1, -2, -3; and then renamed Mage-b1, -b2 and –b3.

Later, twelve murine homologous genes (eight homologues to the MAGEA human gene and four homologues to the MAGEB human gene) were identified. These mouse genes present a chromosomal localisation, a structure and an expression pattern similar to the human genes (Forslund et Nordqvist, 2001).

These findings support that the mouse model represents an attractive tool for studying the functions of type I MAGE genes, as their homologues exist in human.

Expression in male germ cells

Type I MAGE genes are expressed during spermatogenesis (Figure 3). For instance, MAGEA1 and MAGEA4 proteins are expressed in the cytoplasm and the nucleus of spermatogonia and primary spermatocytes, hinting the possible role of these proteins in the early steps of spermatogenesis (Takahashi *et al*. 1995). In mice, Mage-a genes are also expressed in spermatogonia (Chomez et al. 1995). On the other hand, Mage-b proteins were detected in spermatids, post-mitotic cells that will differentiate into spermatozoids (Clotman *et al.* 2000).

Epigenetic regulation, such as methylation, plays a crucial role in spermatogenesis. It has been demonstrated that *de novo* methylation occurs in the pro-spermatogonia. The methylation pattern is completed by the end of the first meiosis (Oakes *et al*., 2007; Carrell *et al.*, 2010). Nevertheless, some genes are expressed early in spermatogenesis but are silenced in the maturing spermatid by gradually acquiring methylation in post-meiotic spermatocytes (Ariel *et al*., 1991, Ariel *et al.*, 1994; Carrell *et al*, 2010).

In view of these observations, a possible hypothesis is that type I MAGE genes, whose expression is controlled by methylation, could play a role at different stages of spermatogenesis.

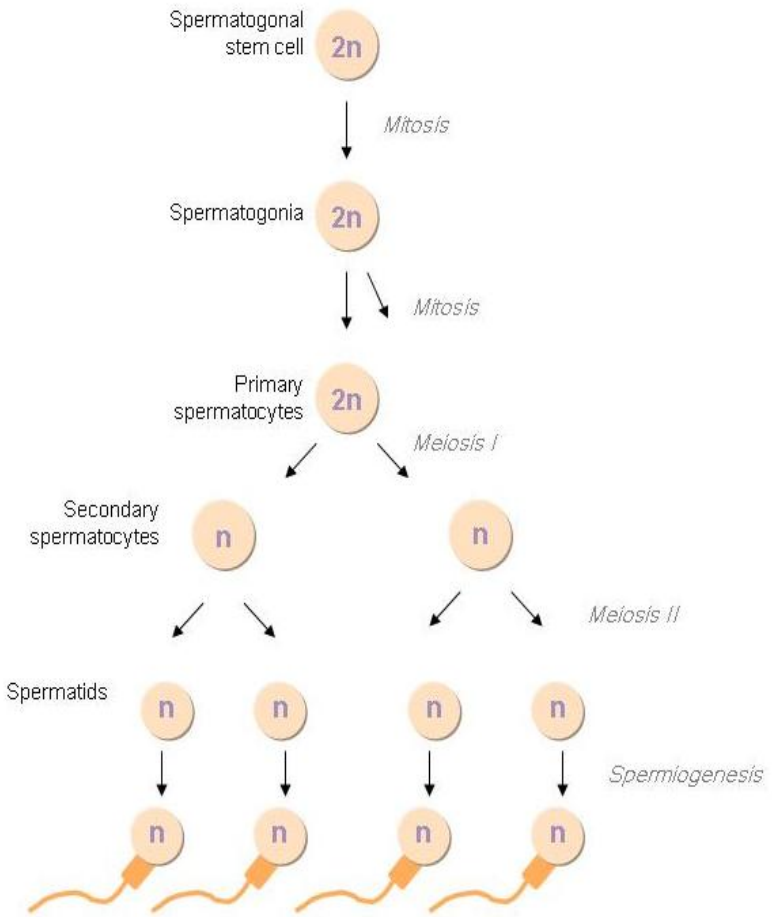

Figure 3: Steps of spermatogenesis. Spermatogenesis takes place in seminiferous tubules in a centripetal cell flow. After proliferation by mitosis, spermatogonia differentiate in primary spermatocytes. The first meiosis allows the generation of secondary spermatocytes and the second gives rise to spermatids. The last step is spermiogenesis, during which round spermatids become spermatozoids freed from the lumen of seminiferous tubules.

2) Roles of type I MAGE genes

Influence of the type I MAGE on the tumor suppressor p53

An interesting aspect about type I MAGE proteins is their influence on the p53 tumor suppressor. The p53 tumor suppressor gene, inactivated in 50% of cancers, is involved in cell cycle progression, apoptosis, senescence, cell migration and invasion (Ladelfa *et al.*, 2012). The mode of action of the p53 tumor suppressor protein is double. First, p53 is a transcription factor able to induce expression of target genes playing a role in apoptosis or in cell cycle control, for instance. Second, the p53 protein also acts at the mitochondrial level by increasing the membrane permeability and by inducing apoptosis through the activation of the caspases cascade.

In normal unstressed conditions, the level of p53 proteins is maintained low through degradation by the E3 ubiquitin ligase MDM2 (Mouse Double Minute 2) (Muller *et al.,* 2011). Moreover, the structural state of p53 prevents its binding on target genes by masking its DNA binding sites. When cells are undergoing cellular stress, such as DNA dammages, p53 protein is stabilized by post-translational modifications in order to play its tumor suppressor role. Interstingly, MAGE genes are able to inhibit p53 activity by three different ways (as summarized in figure 4A).

First, MAGEA proteins interfere with the functions of p53 by interacting with SKIP (Ski interacting protein), an adapter protein essential for the expression of p21. The protein p21 is a target gene of p53 involved in cell cycle progression by inhibition of the Cdk (cycline dependent kinases) (Laduron *et al.*, 2004). Actually, SKIP counteracts the apoptosis mediated by p53 via selective regulation of p21Cip1 mRNA splicing (Chen Y *et al.*, 2011, Zhao *et al*, 2006). On the other hand, MAGEA1 is able to recruit histone deacetylases (HDAC) on p53, leading to inhibition of the p53 transcriptional activity through deacetylation of histones around the DNA binding sites of p53 and deacetylation of the p53 protein itself. These findings could explain why MAGEA provides a survival advantage when expressed in cells treated with p53-dependent DNA-damaging agents, such as etoposide or doxorubicin (Monte *et al.,* 2006).

Another mechanism by which MAGE proteins influence p53 involves RING-containing E3 ubiquitin ligase, a subtype of E3 ligases. E3 ligases are major components of the ubiquitination cascade by binding E2 enzymes coupled to their substrate, leading to the degradation of the substrate in a proteasome-dependent way (Doyle *et al.*, 2010). MAGE proteins interact trough their MHD with RING proteins, without implication of the RING domain. For example, MAGE proteins (specifically MAGEC2, MAGEA2, MAGEA3 et mMageb) are able to bind the TRIM-28 (Tripartite motif-containing 28) protein, also named KAP-1 (Krüppel Associated protein-1), a RING protein that targets p53 for its proteasomal degradation. Doyle and his team demonstrated that MAGE proteins bind and induce a stimulating conformation change of TRIM-28 leading to the degradation of p53 in a proteasome-dependent manner (Figure 4B) (Doyle *et al.*, 2010; Yang *et al*, 2007). Moreover, TRIM-28 joins several other ubiquitin ligases that promote ubiquitin-mediated degradation of p53 including MDM2, another ubiquitine ligase which targets p53. In summary, MAGE genes are able to induce the proteasomal degradation of p53 by stimulating both TRIM-28 and MDM2 proteins.

Finally, MAGEA proteins inhibit the p53-dependant transcription by direct interaction with the DNA binding domain of the p53 core (Marcar *et al.*, 2010). This hypothesis was confirmed by an augmentation of the binding between p53 and its target genes p21, Bax and Puma after MAGE-A genes silencing.

(A)

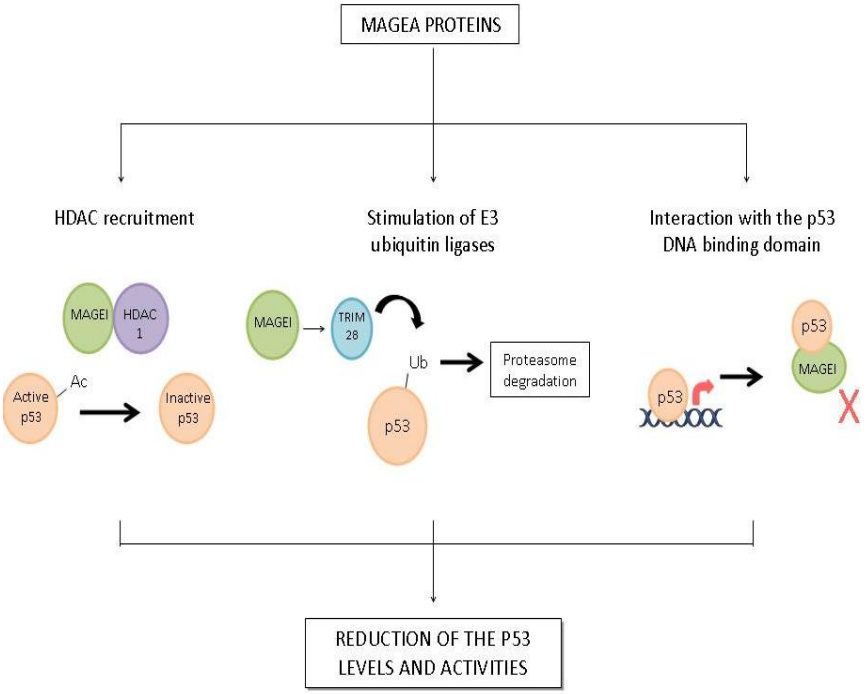

(B)

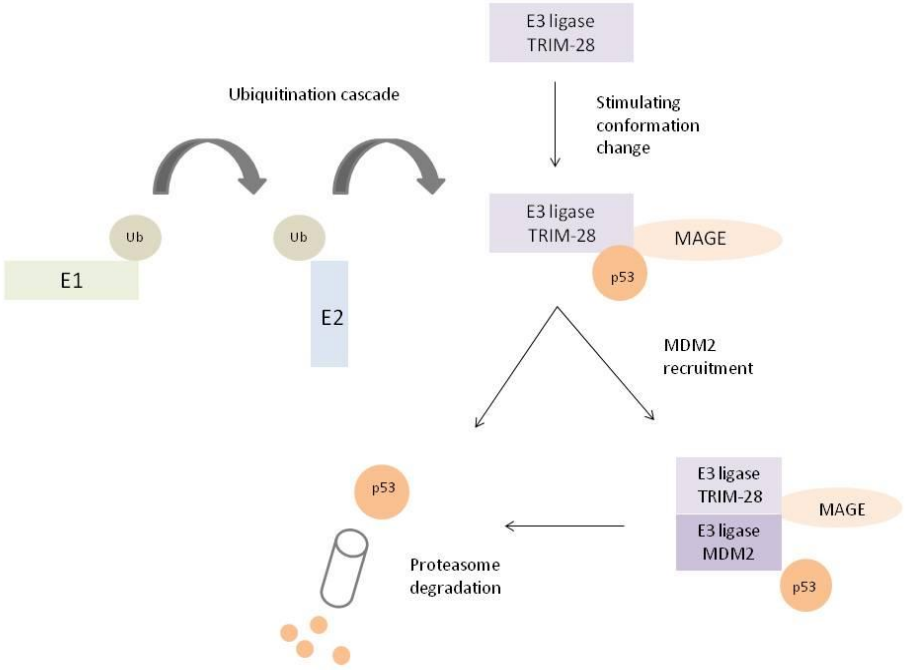

Figure 4: (A) Influence of type I MAGE genes on the tumor suppressor p53. Type I MAGE genes could inhibit p53 by three different ways: (1) By recruitment of HDAC leading to the inactivation of p53 after deacetylation. (2) By stimulation of E3 ubiquitin ligases, among them TRIM28 that induces p53 ubiquitylation and proteasome degradation. (3) By interaction with the DNA binding domain of p53. (B) Illustration of the processus of degradation of p53 through the ubiquitylation cascade. Type I MAGE proteins bind and stimulate the TRIM-28 protein, a E3 ligase containing a RING domain. Once activated, TRIM-28 binds p53, leading to it's degradation in a proteasome dependent manner. TRIM-28 can also recruit MDM2 for the degradation of p53 in the proteasome.

Induction of the hypoxic response

During tumor growth, cells in the center of the tumor become so distant from blood vessels that their environment becomes hypoxic. The hypoxia inductible factor 1 (or HIF-1 factor), a transcription factor induced in hypoxic conditions, is composed of two sub-unit: HIF-1α and HIF-1β (Porporato *et al*, 2011). The β sub-unit is constituvely present in the cell nucleus, while the α sub-unit is only stabilized in absence of oxygen. Effectively, in normoxia, HIF-1α is hydroxylated by the prolyl-hydroxylase PHD2 to be recognized by the VHL (von Hippel Lindau) protein which mediates its degradation in a proteasome-dependent way. In a hypoxic environment, HIF-1α, non hydroxylated by the PHD2, is not directed in the proteasomal pathway. The association of HIF-1α with the β sub-unit leads to the obtaining of a functionnal transcription factor targeting a set of genes involved in the glycolytic switch and angiogenesis.

Interestingly, it has been demonstrated that MAGEA proteins are able to influence this pathway in hypoxic cancer cells. Indeed, MAGEA2, MAGEA9 and MAGEA11 proteins interact and suppress the activity of the prolyl hydroxylase 2 (PHD2), which maintain HIF-α proteins at low levels in normoxic conditions (Aprelikova *et al.*, 2009). This way, MAGEA proteins stabilize the HIF-1α subunit to enhance the hypoxic response.

Inhibition of caspases

Another function of MAGEA genes is their involvement in the onset of apoptosis through inhibition of caspases. For instance, the binding of MAGEA3 protein to the pro-caspase 12, inhibits the activation of caspase 12 involved in endoplasmic reticulum stress (Sang *et al.*, 2010). Tumor cells expressing type I MAGE genes would be protected against such damages, conferring to them a survival advantage (Morishima *et al*, 2002).

Pro-apoptotic activity

Interestingly, the N-terminal truncated form of MAGEA4 was reported to have a pro-apoptotic activity. First, an interaction between MAGEA4 and the gankyrin, an oncoprotein over-expressed in hepatocarcinoma, has been reported. It has been demonstrated that MAGEA4 was able to decrease the oncogenic activity of the gankyrin (Nagao et al, 2003). Second, it has also been observed that MAGEA4 is cleaved by a caspase-dependent protease after DNA damages to generate the MAGEA4ΔN1 fragment. This fragment binds to Miz-1, a zinc finger transcription factor responsible of the inhibition of p21. Once activated, the protein p21 blocks the cell cycle. Moreover, MAGE-A4ΔN1 decreases the Bcl-xL protein level, inducing cell death (Sakurai et *al*., 2004).

V. INVOLVEMENT IN TUMORIGENESIS

Some evidences support the hypothesis that type I MAGE genes could have an active role in cancerogenesis. First, it is demonstrated that some MAGEA proteins confer resistance to chemotherapeutic drugs, as paclitaxel, doxurubicin or etoposide (Duan *et al*, 2003; Monte *et al.*, 2006; Suzuki *et al.*, 2007). Moreover, MAGEA genes expression is associated with tumor invasiveness, lymph node metastasis, poor prognosis and advanced clinical stage (Sang, Wang *et al*, 2011; Jung *et al.*, 2005). The inhibition of the p53 and HIF induction are also consistent with these hypothesis. These findings make the type I MAGE genes an attractive target for immunotherapy.

1) Chemoresistance

Chemotherapy is the major treatment to kill cancer cells, characterized by a high division speed. Chemotherapeutic drugs can be divided in different categories according to their mode of action:

- Antimitotic agents
  The antimitotic agents are so-called because of their ability to interfere with the mitotic spindle. For instance, some chemotherapeutic drugs as paclitaxel or docetaxel are able to destabilize the mitotic spindle by inhibiting the polymerization of tubulin.

- Intercalating agents
  The intercalating agents are able to incorporate the DNA, inducing the blockage of polymerase and of the DNA synthesis. For instance, doxurubicin is an intercalating agent.

- Antimetabolit agents
  The antimetabolit agents work by inhibiting DNA synthesis. The 5-fluorouracil (5-FU) is an example of antimetabolit. 5-FU is an analog of pyrimidin used by the thymidilate cyclase, no more available for thymidine synthesis.

- Topoisomerase inhibitor agents
  The inhibitors of topoisomerase induce the stabilization of the DNA breaks performed by the topoisomease. Etoposide, for example, is able to stabilize double strand breaks generated by topoisomease II.

However, the efficiency of chemotherapy is entraved by the ability of some cancer cells to develop resistance mechanisms to cell death. Intruigingly, type I MAGE genes are reported to participate to cell chemoresistance. Indeed, MAGEA1 expression is correlated with resistance to apoptosis when melanoma cells are treated with classical chemotherapeutic drugs, as paclitaxel, doxurubicin or etoposide (Duan *et al*, 2003; Monte *et al.*, 2006; Suzuki *et al.*, 2007). Our lab previously demonstrated a chemoresistance of MCF-10A cells expressing MAGEA1 (Elise Srour, unpublished data). The tested drugs were etoposide, 5-fluorouracil and docetaxel. Etoposide and 5-fluorouracil are reported to work through a p53-dependent manner, but not docetaxel. This observation suggested the involvement of a p53-independent mechanim of chemoresistance induced by MAGEA1.

Such a mechanism could involve ATP-binding cassette (ABC) transporters, major mediators of multidrug resistance (Ansbro *et al.*, 2013, Gillet and Gottesman, 2012). ABC transporters mediate the efflux of several compounds through cells or organelles membranes. They act as keepers of the organism by regulating the permeability of several organic barriers, as the blood-brain barrier, testis, placenta, kidney, liver and gastro-intestinal tract. This way, ABC transporters control the excretion of toxins to protect the cells. Nineteen genetic diseases have been reported to be associated with mutations in these genes. ABC genes are also well known for their role in allowing cancer cells to evade response to treatment through efflux of chemotherapeutic drugs (Ansbro *et al.*, 2013, Gillet and Gottesman, 2012).

2) Cell migration and invasion

It has been demonstrated that the expression of type I MAGE genes is associated with advanced clinical stage in melanoma. Effectively, Barrow and his team discovered that the frequency of MAGEA1 expression in primary melanoma was 20% and increases up to 51% in distant metastasis (Barrow *et al*, 2006). These results were consistent with those obtained by Brasseur *et al*, who reported that MAGEA1 was expressed in 16% of primary melanomas and 48% of metastatic melanomas (Brasseur *et al*, 1995). These results suggest an acquisition of the MAGEA1 antigen with progressive stage of cancer, as in thicker and ulcerated melanomas.

Another study published in 2013 showed that the forced expression of MAGEA3 resulted in p21 down-regulation, accelerated cell cycle progression but also in cell migration and invasion (Liu *et al*, 2013). Firstly, *in vitro* studies, consisting in scratch tests and tridimensional matrigel chambers were performed. Scratch tests involve performing a wound in a cell monolayer in order to observe the time take by cells to invade the scratch (see *Materials and Method* for details). The matrigel chamber is another method used to study cell migration by reconstituting the basal membrane *in vitro*. Actually, the invasive cells are able to pass through the membrane by secretion of proteases, while the non-infiltrative cells will stay in the first compartment. These two *in vitro* assays revealed that MAGEA3 significantly promotes cell migration and invasion (Liu *et al*, 2013). Furthermore, the team also proves that MAGEA3 enhances thyroid tumor growth and lung metastasis *in vivo* by using a mouse model injected by MAGEA3-positive cells.

These findings suggest that several MAGE proteins can be involved in migration and invasion of cancerous cells. It implies that MAGE antigens could be used as prognosis marker or targets for immunotherapy.

3) Immunotherapy

In an experiment performed fifty years ago, mice with malignant tumors were treated by surgical excision of the tumor. When these mice were injected with cells from the excised tumor, they did not develop the tumor again. This experiment raised the hypothesis that tumor cells present specific antigens able to induce an immune response. This finding was the observation indicating that immunotherapy in the treatment of cancer could be effective. The purpose is to stimulate the immune system against tumor cells (Van Pel *et al*, 1992).

As mentioned above, the specific expression of MAGE proteins in cancer cells makes them an attractive target for immunotherapy. Male germ cells do not express HLA, which ensures a specific immunogenic targeting of cancer cells (Sang *et al.*, 2010). Several methods are conceivable to target MAGE antigens in immunotherapy (Gillespie & Coleman 1999; Caballero & Chen 2009):

- A first approach is the direct vaccination of the patient with MAGE peptides
- A second method consists to vaccinate the patient with cancer cells expressing MAGE peptides at their surface
- Finally, it is also possible to inject antigen-presenting cells (APC) of the patient cultivated in presence of MAGE peptides to stimulate T cells.

MAGE peptides are currently being investigated as immunizing agents in clinical trials. These studies are showing encouraging results for gastro-intestinal cancers, oesophagus carcinomas, lung carcinomas and melanomas (Bhutani *et al.*, 2011; Forslund et Nordqvist, 2001). Specifically, a MAGEA3 vaccine is tested in phase 3 as adjuvant therapy for lung cancer and melanoma (Marchand *et al*., 1995; Brichard *et al*., 2013).

VI. METHODS OF TRANSGENESIS

One of the goals of my project is to generate and characterize MAGEA1 transgenic mice. The purpose is to study the involvement in tumor development, chemoresistance and development of metastasis *in vivo*. For this reason, I detailed in this paragraph the two common methods of mouse transgenesis. Table 1 compares the advantages and disadvantages of the two methods.

The first method is additive transgenesis. The DNA is directly injected in mouse blastocysts where it integrates the genome randomly. The mechanism of integration of the transgene into chromosome of zygotes by microinjection in the male pronucleus is not well characterized. Hypothesis is that the introduction of DNA could induce enzymatic activities of DNA repair in the genome of the embryo. Afterwards, zygotes are transferred into the oviducts of surrogate mothers.

The second method is the targeted transgenesis (the “knock-in” method), consisting in modifying a genomic sequence in a chosen integration site. Embryonic stem cells (ES cells), that are totipotent cells isolated from the inner cell mass of the blastocyst, are used in this technology. ES cells can be genetically modified *in vitro* by electroporation or by retroviral infection. The transgene is integrated in the genome of ES cells by homologous recombination. Selected genetically modified ES cells are injected in blastocysts, then implanted in a pseudo-pregnant mouse. The development of the blastocyst will give rise, in 50% of the cases, to a chimeric mouse. The transgene can then transmit to the following generation to establish a lineage of transgenic mice.

Table 1

Additive transgenesis

Advantages	Disadvantages
Faster than targeted transgenesis	Random integration site (coding or no coding sequence)
Any DNA sequence can be injected (BAC, YAC, plasmid)	Efficiency of 3 to 10%
	High levels of technicality of the experimenter
	Integration can induce deletions, duplication, translocation
	Copy number of the transgene is often >1

Targeted transgenesis

Advantages	Disadvantages
In vitro selection of ES cells (for the site of integration, the transgene copy number, karyotype)	Slower than additive transgenesis
Choice of the integration site	Heavy method
No limitation of size	Positive selection marker required

VIII. OBJECTIVES AND WORKPLAN

Type I MAGE genes could play an active role in tumorigenesis, chemoresistance or metastasis. In this work, we explored the possible role of MAGEA1 in tumorigenesis, using a series of *in vivo* and *in vitro* models (Figure 5). Transgenic mice ectopically expressing MAGEA1 were generated in order to assess the effect of MAGEA1 expression on tumor incidence and agressiveness *in vivo*. In parallel, we investigated p53 dependent and independent oncogenic functions of MAGEA1 *in vitro* with a particular focus on cell chemoresistance and migration.

IN VIVO

Direct transgenesis → TYRP-MAGEA1 transgenic mice

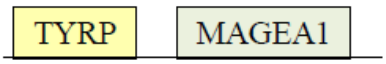

Targeted transgenesis → Rosa26MAGEA1 transgenic mice

IN VITRO

	p53 WT model	**p53 deficient model**
Chemoresistance	MCF-10A; MCF-7	Hep3B
ABC transporters expression	MCF-10A	Hep3B
Migration	MCF-10A	Hep3B

Figure 5: Objectives and workplan. *In vivo* studies consisted in the generation of two MAGEA1 transgenic mice. The first mouse, named TYRP-MAGEA1 transgenic mouse, was obtained by additive transgenesis. The MAGEA1 cDNA was placed under control of the tyrosinase promoter, which is specific for melanocytes. The second mouse, the Rosa26-MAGEA1 transgenic mouse is an inducible mouse model that was obtained by targeted transgenesis. In this model, the induction of MAGEA1 expression is dependend on the excision of the STOP cassette located between the CAG promoter and the MAGEA1 coding sequence. The STOP cassette, flanked by lox sites, can be excised by crossing the Rosa26-MAGEA1 transgenic mice with mice expressing the Cre-recombinase. The *in vitro* studies focused on chemoresistance assays performed with p53 proficient (MCF-10A and MCF-7) and p53 deficient (Hep3B) cells. Expression of ABC transporters was monitored in MCF-10A and Hep3B cells. Finally, scratch tests were performed in order to evaluate the effect of MAGEA1 on cell migration in MCF-10A cells and in Hep3B cells.

MATERIALS AND METHODS

I. pINSULATOR-TYRP-MAGEA1 PLASMID DESIGN

The TYRP-MAGEA1 construct was linearized using BamHI and NotI restriction enzymes. On the other hand, the *pcDNA1-MAGEA1* plasmid was digested with the same enzymes to recover the MAGEA1 insert. After 1 hour of incubation at 37°C, the products of the two digestions were analyzed by a gel electrophoresis on 1% agarose gel in Tris-acetate buffer supplemented with ethidium bromide.

Wizard SV Gel and PCR Clean-UP System (PROMEGA, A9281) kit was used to recover DNA from the gel. To allow ligation, the vector was dephosphorylated with Shrimp Alkaline Phosphatase (SAP) (NEW ENGLAND BIOLABS) in a total volume of 100µl. After 1 hour of incubation, the sample was treated with 1µl of EDTA 0,5M and heated at 70°C for 10 minutes in order to inactivate the enzyme. The mixture was extracted with one volume of phenol-chlorophorm and centrifuged at 14000g for 15 minutes. DNA was then precipitated in 2,5 volumes of ethanol 100% after adding 0,1 volume of sodium acetate (NaAc) 3M. After one hour of incubation at -80°C, the sample was centrifuged at 14000g for 10 minutes generating a pellet that was washed with 70% ethanol. After air-drying, the DNA pellet was diluted in distilled water.

The dephosphorylated linearized vector and the MAGEA1 insert in a 1:3 proportion were ligated by mixing 400000U/ml T4 DNA ligase (NEW ENGLAND BIOLABS M0202S) and 2µl ligase buffer. The ligation mixture was incubated overnight at 16°C. The next morning, 50µl of DH5-α electro-competent bacteria were mixed with 2µl of the ligation product. Transformed bacteria were then spread onto LB agar treated by 50mg/ml ampicilin in a Petri dish and grown overnight at 37°C. For screening, PCR was performed with primers specific for MAGEA1 gene. The PCR program used was: 5 minutes at 95°C, 30 seconds at 95°C, 30 seconds at 57°C, 1 minute at 72°C and 5 minutes at 72°C. Second, third and fourth steps were performed thirty times.

II. MICE GENOTYPING

Candidate transgenic mice obtained by pronucleus micro-injection were screened by PCR for the presence of the MAGEA1 transgene in their genome. DNA was extracted from a little piece of the tail. Tissue was treated with 200µl lysis buffer (containing 100 mM TrisHCl pH 8, 500mM KCl and 10% Tween 20). After heating 5 minutes at 95°C, 10µl of proteinase K (20mg/ml) was added to the samples and incubated overnight at 55°C.

Proteinase K was inactivated by heating 5 minutes at 94°C. After 10 minutes of centrifugation at 13000g, 1 µl of the supernatant and MAGEA1-specific primers were added to PCR mix. The PCR program used was 5 minutes at 94°C, 30 cycles of [30 seconds at 94°C/30 seconds at 57°C/1 minute at 72°C], a final elongation step of 5min et 72°C terminated the reaction.

III. CELL CULTURE

All cells were cultivated in a humidified incubator at 37°C and 5% CO_2. Regular cell passage was required to avoid contact inhibition and to provide new nutriments. To this end, cells were washed with phosphate buffer saline (PBS) (LONZA, BE17-516F) to eliminate dead cells, debris and any residual medium. Trypsin-EDTA (LONZA, BE17-161^E) was then added in order to detach cells from the dish. After a few minutes at 37°C, complete medium was added to the trypsinized cells and an appropriate number of cells were collected and adequately diluted on a new support. Cells were resuspended in Trypan Blue (ratio 50:50) to stain non viable cells and transferred to a KOVA counting chamber. Cell concentration was determined as follows: Cell concentration (cell number/ml) = counted cell number x 2 (dilution factor) x 1000.

Hep3B cells

The Human Hepatoma cell line Hep3B is derived from a human hepatocellular carcinoma. Hep3B cells are deficient for p53. For this reason these cells were used to study p53-independent mechanisms. Hep3B cell line was cultivated in Dulbeco's Modified Eagle Medium (DMEM 1X) (LONZA, BE12-604F) supplemented with 10% Fetal Bovine Serum (FBS) (LONZA, DE14-801F) and 1% penicillin/streptomycin (LONZA, DE17-602E).

MCF-10A cells

MCF-10A cell lines are mammary epithelial cell lines untransformed but spontaneously immortalized (Soule *et al*, 2010). MCF-10A cells were cultivated in DMEM/F12 (1:1) 1X (GIBCO, 11320-074) medium supplemented with 5% horse serum (HS) (GIBCO, 26050-088), 1% of penicillin/streptomycin, 10µg/ml of insulin (SIGMA ALDRICH, I9278-5ML), 100ng/ml of choleric toxin (SIGMA ALDRICH, C8052-1MG), 500ng/ml of hydrocortisone (SIGMA ALDRICH, H0396-100MG) and 20ng/ml of human epidermal growth factor (hEGF) (SIGMA ALDRICH, E9644-2MG

MCF-7 cells

MCF-7 cells, a human epithelial cell line, was the first mammary cell line cultivated for a long term. MCF-7 cells were cultivated in DMEM 1X, 10% FBS and 1% of penicillin/streptomycin and 15nM Hepes.

293T cells

293T cells, derived from Human Embryonic Kidney (HEK) were used for lentiviral packaging. The 293T cell line was cultivated in the same standard medium (DMEM 1X, 10% FBS and 1% penicillin/streptomycin), supplemented by glutamax 100X and 0,6mg/ml of glucose before transfection.

B16 cells

B16 melanoma cells are obtained from a mouse melanoma (C57BL/6J). This cell line is a suitable transfection host. The B16 cell line was cultivated in DMEM 1X, 10% FBS, 1% penicilin/streptomycin and glutamax 1X.

IV. CALCIUM-DEPENDENT TRANSFECTION AND CELL TRANSDUCTION

293T cells, derived from human embryonic kidney cells (HEK293), were used to produce lentiviral particles. On the first day, 293T cells were enumerated and 1,3 million cells were plated in a T25 flask. Before transfection, the cell medium (DMEM1X, 10%FBS, 1% penicillin/streptomycin) was supplemented with glutamax 1x and 0,6mg/ml of glucose. Cells were transfected with two different lentiviral vectors: (1) a vector expressing MAGEA1 and (2) an empty vector, as a negative control.

One day later, once cell confluence reached 30-40%, mixtures were prepared to allow calcium-dependant transfection and viral particles production. These mixtures, adapted for a T25 flask, consisted of 500µl HBS 2X, 62,5µl CaCl 2M, 3,5µg of the lentiviral vector for the calcium-dependant transfection. In order to package and produce viral particles, 1,25µg pMDLg/PRRE, 1,25µg pRSV-Rev and 1,25µg VSVg vectors (ADDGENE), coding for gag, env and rev genes, were added to the mixture. Mixtures were then added to the cells.Two days after transfection, the supernatant containing viral particles was collected and centrifuged 5 minutes at 12000g and filtered through a 0.45µ filter (MILLIPORE, MA01730) and frozen at -80°C.

Cell infection was performed by addition of viral particles (1,5ml per T25 plate) and polybrene 5µg/ml (CHEMICON INTERNATIONAL, TR-1003-G). After eight hours of incubation, cell culture was diluted in standard medium. A dose curve was carried out to establish neomycin concentration for cells selection.

V. WESTERN-BLOT

To obtain protein extracts, the cells were first rinsed with PBS 1X and treated with lysis buffer 1X (0.05 M Tris pH 8, 0.15 M NaCl, 0.005 M EDTA, 1% Nonidet P40 and 0.5% sodium desoxycholate) with a protease inhibitor cocktail diluted 100X (Proteoblock). After ten minutes of incubation on ice, cell membranes were degraded, thereby freeing cytoplasmic and nuclear proteins. The supernatant was cleared by a centrifugation during 15 minutes at 14000g at 4°C. Concerning mice protein lysates, the organs were first dissected, weighted then grinded in lysis buffer 1X (10X the volume of the weight of the organ). The samples were incubated twenty minutes on ice. After vortexing, samples were centrifuged 15 minutes at 14000g at 4°C.

The Pierce BCA Protein Assay Kit (THERMO SCIENTIFIC 23225) was used to determine protein concentrations of the lysates by densitometry. Protein concentrations were determined on basis of a standard growing concentration of BSA (Bovine Serum Albumin). Fifteen to thirty micrograms of proteins were mixed with 5µl of Laemmli buffer 5X (0.5 SDS, 10% glycerol, 6.25 mM Tris pH 6.8 0.003% bromophenol blue and 25 mM DTT (dithiothréitol)) and distilled water to reach a total volume of 25 µl. The sample was heated at 95°C during 5 minutes to denature proteins.

Proteins were migrated onto an SDS-PAGE gel (sodium dodecyl sulphate polyacrylamide gel electrophoresis), composed of a stacking gel - to assemble samples before migration - and a migration gel, separating proteins according to their molecular weight. Proteins were then transferred onto PVDF (Polyvinylinedifluoride) membranes. After protein transfer during 1.5 hours, PVDF membranes were blocked for 30 minutes with a buffer made

of PBS 1X, 0.05% of Tween 20 and 5% of powdered milk. Membranes were then incubated in primary antibody diluted in PBS 1X, 0.05% Tween 20 and 1% milk at 4°C overnight. After three washes of 10 minutes in PBS 1X, Tween 20 0.05%, membranes were incubated in the adapted secondary antibody, conjugated with the Horseradish Peroxydase (HRP), allowing revelation by chemoluminescence (Polyclonal Goat Anti-Mouse Immunoglobulins/HRP DAKO P0447; Polyclonal Goat Anti-Rabbit Immunoglobulins/HRP DAKO P0448). After three additional washes, HRP substrates (Supersignal West Pico Chemiluminescent Substrate THERMO SCIENTIFIC 34095; Supersignal West Femto Maximum Sensitivity Substrate THERMO SCIENTIFIC 34080) were added to the membranes. Proteins could then be revealed by autoradiography.

VI. REVERSE TRANSCRIPTION AND QUANTITATIVE PCR

After washing with PBS 1X, cells were collected in 1ml of TRI-Reagent™ for a cell pellet of 5 to 10.10^6 cells. The resulted cell lysate was centrifuged at 12000g for 10 minutes at 4°C. After treatment with chloroform (200µl chloroform per mL of TRI-Reagent™) and vortexing, an emulsion was obtained. After an incubation of 15 minutes, an additional centrifugation allowed formation of three distinct phases: red organic phase (containing proteins), interphase (DNA) and aqueous phase (RNA). The aqueous phase was collected and precipitated in isopropanol (500µl per of TRI-Reagent™). The pellet was washed by ethanol 75% and diluted in 25µl of distilled water. Concentration and purity of the extracted RNA were measured through optic density by the Nanodrop Spectrophotometer. The extraction of RNA from mice was performed in a slightly different way. Organs were collected and grinded in 10 volumes of TRIzol. After adding 200µl of chlorophorm, the tube was shaken vigorously by hanging inversion. After 5 minutes of incubation at room temperature, samples were centrifugated 15 minutes at 4°C and at 12000g allowing the formation of three distinct phases: red organic phase (containing proteins), interphase (DNA) and aqueous phase (RNA). Next steps were performed in the same manner than with cell extracts.

The *SuperScriptTM II Reverse Transcriptase kit* (INVITROGEN, 18064-014) was used to perform reverse transcription. To this end, 1µg of RNA was mixed with 1µl dNTP Mix 10mM (INVITROGEN, 18427-013), 1µl Random Hexamer Primer (FERMENTAS, S0142) and 12µl DEPC water. After a five minutes heating at 65°C, 40U/µl of enzyme RNAse and 4µl buffer *First-Strand 5X* were added to each sample. These samples were then treated 10 minutes at 45°C, 30 minutes at 50°C and 5 minutes at 85°C to inactivate the enzyme. After diluting the cDNA in 40µl DEPC water, samples were analyzed by the Nanodrop Spectrophotometer to evaluate cDNA concentration.

The last step was the quantitative PCR allowing us to estimate genes expression in different conditions, in comparison with a housekeeping gene. To this end, cDNA is mixed with 2,4µM primer forward, 2,4µM primer reverse and 10µl *SYBR Green/ROX qPCR Master Mix* (containing the DNA polymerase, dNTP in adequate buffer, a colouring agent SYBR Green and the passive colouring agent ROX) *(*MOLECULAR RESEARCH CENTER TR118). The PCR program was included 2 minutes at 50°C, 10 minutes at 95°C, 40 fold 15 seconds at 95°C and 2 minutes at 60°C. Data analysis was performed by the *7300 System* software. To interpret results, we calculated ΔCt to normalized genes expression according to the housekeeping gene (GADPH) and the ΔΔCt to compare our results between our control and tested samples.

VII. MTT TEST

The MTT test was used to evaluate growth and cell viability, through a measure of cell metabolism. MTT, or 3-(4,5-dimethylthiazol-yl)-2,5-diphenyltetrazolium bromide (SIGMA ALDRICH, M2128-1G), can be transformed by mitochondrial reductases in a substance generating purple crystals. This reaction can only be performed in active metabolic cells, giving an idea of cell viability. Absorbance of purple crystals was measured by a spectrophotometer. Cells were cultivated in a 24-wells plate (50,000 cells per well) in an adequate culture medium.

The next day, cell medium was replaced by new medium containing chemotherapeutic agents as etoposide (SIGMA ALDRICH, E1383-25MG), docetaxel (SIGMA ALDRICH, 01885-5MG-F) or 5-fluorouracil (SIGMA ALDRICH, F6627-1G). After different post-treatment times, each well was treated with 500 µl of MTT solution (2,5mg/ml PBS) and incubated for two hours. Five-hundred microliters of DMSO (dimethylsulfoxyde) was added in each well before an additional incubation of one hour. To finish, cell absorbance was determined by spectrophotometry.

VIII. SCRATCH TEST

The scratch test is a common and easy technique to study cell migration. The test starts with the creation of a wound in the cell monolayer. Actually, once cells reach confluence in a Petri dish (of sixty millimetres), the wound is performed using a tip of a p200 pipette. Cells migrate to close the wound and restore cell contact. After changing the medium by medium deprived with serum (DMEM, FBS 0,1%, PS 1%), several pictures are taken, at time zero and at different intervals after the scratch.

This way, it is possible to study and compare the migration rate of different cells types.For each interval, three scratches are performed (left-medium-right segments) and for each of these, three points are photographed (top-medium-bottom points). Marks on the Petri dish allow photography of these same points in time. A software of image processing (PhotoFiltre 7) make de measure of the wound possible. Afterwards, the quantification of the scratch test was carried out by calculating the opening percentage of the scratch:

$$\text{Opening percentage} = \frac{\text{Average opening at time T0}}{\text{Average opening at time T1}} \times 100$$

RESULTS:

IN VIVO MODELS

I. ADDITIVE TRANSGENESIS: THE TYRP-MAGEA1 TRANSGENIC MICE

1) The TYRP-MAGEA1 transgene

One of the goals of our work is to study the involvement of MAGEA1 in tumorigenesis using *in vivo* models (Figure 5). For this reason, the lab started the construction of transgenic mice ectopically expressing MAGEA1 in melanocytes. These mice were obtained by additive transgenesis (Figure 6). The global strategy was to clone the MAGEA1 coding sequence under control of the tyrosinase promoter (TYRP), specific for melanocytes. The TYRP-MAGEA1 cassette was flanked by insulators sequences, which should help to protect the transgene from the possible spreading of neighbouring heterochromatin and of the activity from distally located enhancers (West AG, Gaszner M and Felsenfeld G, 2002).

The MAGEA1 cDNA was inserted into a plasmid named TYRP-plasmid, under control of the tyrosinase promoter. This tyrosinase promoter, specific for the melanocyte lineage, was used to drive MAGEA1 expression specifically in melanocytes. (Figure 6A-B-C) (Delmas *et al*, 2007). The MAGEA1 cDNA was inserted between the BamHI and NotI restriction sites in the TYRP-plasmid, the recombinant plasmids were analyzed by restriction and PCR (Figure 6D-E). The ability of this construct to drive the expression of MAGEA1 in melanoma cells was evaluated by western-blotting after transient transfection of B16 melanoma cells. Results presented in Figure 6F indicate that the vector efficiently induced the expression of MAGEA1 in B16 cells.

The next step was to transfer the *TYRP-MAGEA1* cassette between the ClaI and NotI restriction sites, located in the *pInsulator* vector (Figure 6G-H). This way, the transgene was flanked by insulators sequences to obtain a protection from undesirable regulations. The structure of the construct *pInsulator-TYRP-MAGEA1* was validated by PCR and restriction analysis with SalI and FseI (Figure 6I-J-K). Results show an efficient linearization of *pInsulator-TYRP-MAGEA1* by FseI. Double digestion by FseI and SalI generated two fragments, one of which corresponds to the fragment of interest that will be purified and injected in the pronucleus of mouse zygotes.

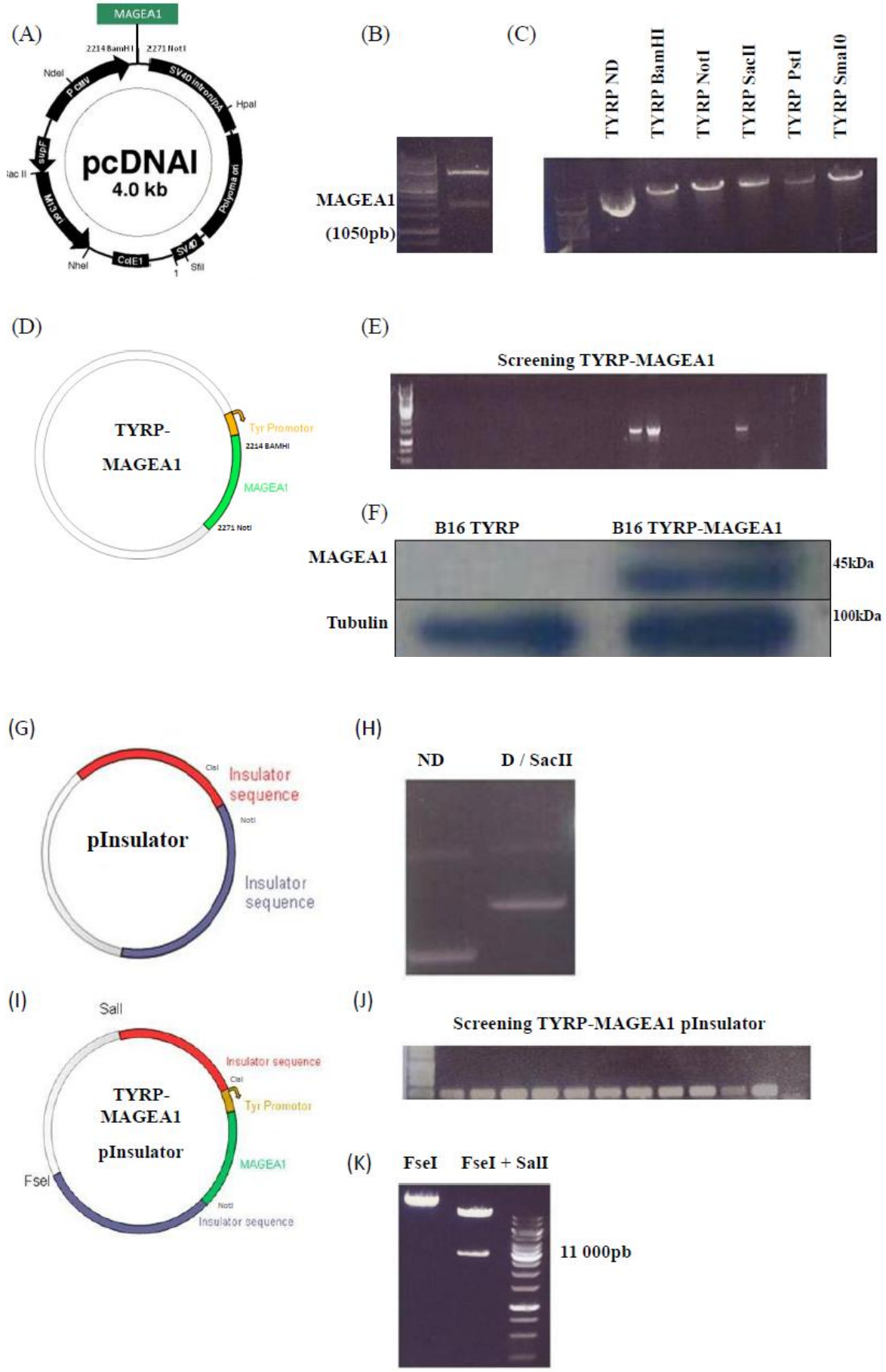
(A)
MAGEA1
2214 BamHI
2271 NotI
NdeI
P cmv
SV40 intron/pA
HpaI
pcDNAI
4.0 kb
SV40
Polyoma ori
CoIE1
NheI
SfiI
(B)
MAGEA1
(1050pb)
(C)
TYRP ND
TYRP BamHI
TYRP NotI
TYRP SacII
TYRP PstI
TYRP SmaI0
(D)
TYRP-
MAGEA1
Tyr Promotor
2214 BAMHI
MAGEA1
2271 NotI
(E)
Screening TYRP-MAGEA1
(F)
B16 TYRP
B16 TYRP-MAGEA1
MAGEA1
45kDa
Tubulin
100kDa
(G)
ClaI
Insulator sequence
NotI
pInsulator
Insulator sequence
(H)
ND
D / SacII
(I)
SalI
Insulator sequence
ClaI
TYRP-
MAGEA1
pInsulator
Tyr Promotor
MAGEA1
FseI
NotI
Insulator sequence
(J)
Screening TYRP-MAGEA1 pInsulator
(K)
FseI
FseI + SalI
11 000pb

Figure 6: (A) Plasmid map of pcDNA1 containing the MAGEA1 cDNA located between BamHI and NotI restriction sites (B) Electrophoresis gel analysis of the pcDNA1-MAGEA1 digestion with BamHI and NotI (C) Electrophoresis gel analysis of the TYRP plasmid digestion: ND (non-digested) or digested by BamHI, NotI, SacII, PstI, SmaI enzymes (D) Plasmid map of TYRP-MAGEA1 plasmid (E) PCR screening on colonies susceptible to contain TYRP-MAGEA1 plasmid (F) Western-blot analysis of proteins extracted from B16 cells transiently transfected with TYRP-MAGEA1 plasmid or empty TYRP plasmid, as negative control. Tubulin, a structural protein of microtubules, is used as loading control (G) Plasmid map of pInsulator plasmid (H) Electrophoresis gel analysis of the pInsulator plasmid digestion: ND or disgested by SacII enzymes (I) Plasmid map of pInsulator-TYRP-MAGEA1 (J) PCR screening of colonies susceptible to contain the TYRP-MAGEA1 pInsulator-plasmid (K) Electrophoresis gel analysis of the pInsulator-TYRP-MAGEA1 plasmid digestion with FseI or with FseI and SalI restriction sites.

2) GENERATION OF TYRP-MAGEA1 TRANSGENIC MICE

Having obtained the derived TYRP-MAGEA1 construction, the next step was to generate MAGEA1 transgenic mice by additive transgenesis. Oocytes were recovered from mated mice and TYRP-MAGEA1 DNA was directly injected in the male pronucleus. Injected eggs were then implanted into the oviduct of pseudo-pregnant mice (work performed by Dr Younes Achouri, UCL).

We obtained a total of 64 mice that were genotyped using a PCR specific for MAGEA1. Nine of these mice were MAGEA1 positive and used as founders of the transgenic lineage (Figure 7). The founders were mated with wild-type mouse (C57B6) to determine if the MAGEA1 transgene could be transmitted to the progeny. The percentage of transmission was estimated to approximately 25%.

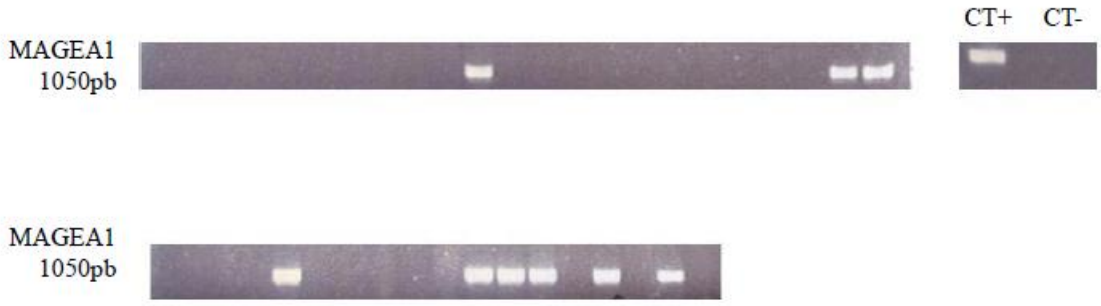

Figure 7: PCR genotyping of DNA extracted from mice tail (mice 0 to 64). Positive control corresponds to pcDNA3-MAGEA1 while distilled water replaces DNA for the negative control.

3) CHARACTERISATION OF TYRP-MAGEA1 TRANSGENIC MICE

The next step after obtaining MAGEA1 transgenic mice was to characterize expression of MAGEA1 in each of the mice lineages. Each founder and its lineage could be different according to the site of integration, the transgene copy number and MAGEA1 expression.

In order to determine the expression of MAGEA1 in TYRP-MAGEA1 transgenic mice, western-blot analyses were performed on proteins extracted from skin of three different TYRP-MAGEA1 transgenic mice lineages (lineages n°1, n°2 and n ° 3) (Figure 8). The skin of a wild-type mouse was used as negative control (CT-). Proteins extracted from MCF-7 ^{MAGEA1} were employed as a positive control (CT+). The antibody anti-MAGEA1 6C1 was used to detect the MAGEA1 protein. This mouse monoclonal antibody reacts broadly with different members of the MAGEA family (MAGEA-1, -2, -3, -4, -6, -10 and 12). The western-blotting, performed with a polyclonal goat anti-mouse immunoglobulin conjugated to HRP (horseradish peroxydase), revealed a band of approximately 50kDa. This result was interpreted as aspecific, given that the band was also detected in the negative control (Figure 8A). The experiment was reiterated using the CleanBlot secondary antibody, allowing the detection of immunoblotted target protein bands without interference with immunoglobulin heavy chains (MW: 49.7 kDa). However, no MAGEA1 protein could be detected in any TYRP-MAGEA1 mice, except with the positive control, suggesting that the first blot detected the immunoglobulin heavy chains of mouse tissues (Figure 8B). A possible explanation is that the level of MAGEA1 transgenic protein could be insufficient to be detected by western-blot analysis, a situation often observed in transgenic mice.

To solve this problem, quantitative PCR following reverse transcription was performed in order to quantify the MAGEA1 mRNA copies in four different mice of each lineage (Figure 9). The number of cycles (Ct) was normalized with regard to a housekeeping gene, the GAPDH (glyceraldehydes-3-phosphate). This way, we obtained a value of ΔCt allowing us to calculate the fold change ($2^{-\Delta\Delta Ct}$) and, by that MAGEA1 relative expression. Figure 9 represents the expression of MAGEA1 in the skin of four TYRP-MAGEA1 mice from different lineages (lineage n°1, n°2, n°3, n°4). Skin from a MAGEA1 negative mouse was used as negative control. Preliminary results acquired from four different mice lineages revealed a transcription of MAGEA1 at different levels in the skin. The relative expression was determined by calculating a percentage of fold change, compared to a maximum fold change (100%). The maximum fold change was attributed to the mouse n°1, which presents the highest expression of MAGEA1. The mouse of the lineage n°2 presents a number of transcripts of 66% compared to the mouse n°1 (100%). For mice lineages n°3 and n°4, the percentage of transcripts were respectively 3,8% and 1,4%. We also performed quantitative RT-PCR analyses on other organs: testis, heart, brain and liver. The skin of mice 1 was used as positive control. Organs of a wild-type mouse were employed for negative controls. No MAGEA1 transcript was detected either in testis, heart, brain or in liver. These results raised the hypothesis that MAGEA1 is expressed specifically in the skin but not in other organs of the transgenic mouse, just as expected. Nonetheless, further analyses on other TYRP-MAGEA1 tissues are needed to confirm this hypothesis.

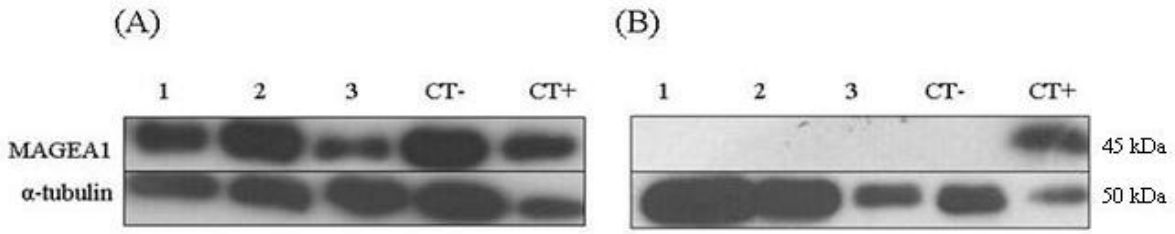

Figure 8: Western-blot analysis of proteins from TYRP-MAGEA1 transgenic mice after revelation with (A) the HRP-coupled polyclonal goat antibody and with (B) the CleanBlot Detection Reagent.

Relative expression of MAGEA1 in the skin of TYRP-MAGEA1 mice

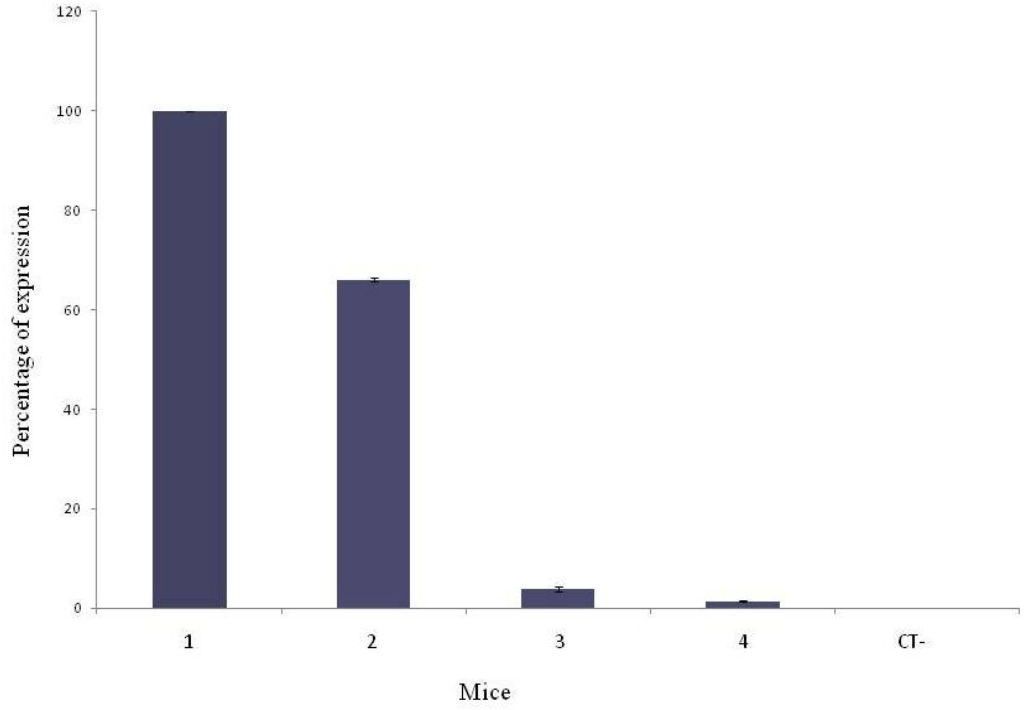

Figure 9: Quantitative PCR analysis following reverse transcription. Relative expression of MAGEA1 in the skin of different TYRP-MAGEA1 mice coming from four different lineages (lineages n°1, n°2, n°3 and n°4). Skin of mouse lineage n°1 was used as reference (100%), as it corresponds to the highest expression of MAGEA1. Negative controls correspond to a wild-type mouse. Error bars correspond to standard deviation for n=2.

II. TARGETED TRANSGENESIS: THE ROSA26-MAGEA1 TRANSGENIC MICE

In parallel to the TYRP-MAGEA1 transgenic mice obtained by additive transgenesis, our lab developed MAGEA1 transgenic mice by targeted recombination. The MAGEA1 insert was cloned in the Ai6 plasmid (Figure 10A) (Madisen *et al*, 2010). The vector contain the MAGEA1 coding region under the control of the CAG promoter, a strong promoter often use to induce a high transgene expression. A *STOP* cassette flanked by lox sites is inserted between the MAGEA1 coding region and the promoter, preventing the expression of MAGEA1. The construction was electropored in embryonic stem cells (ES cells). Genetically modified ES cells were injected in blastocysts and re-implanted in a surrogate mouse.

Twenty-six chimeric mice were obtained and genotyped by a PCR specific for MAGEA1 (Figure 10B). Nine chimeric mice (namely 7 males and 2 females) were found to be MAGEA1 positive and used as founders. These chimeric mice were mated with wild-type mice (C57B6) and the obtained pups were genotyped. Specific PCR to MAGEA1 revealed that five mice among thirteen were positive (Figure 10C). These MAGEA1 transgenic mice should not express MAGEA1, as its expression is prevented by the *STOP* cassette.

These Rosa26-MAGEA1 transgenic mice are currently mated with mice expressing the Cre recombinase. Some of the pup mice would contain both the MAGEA1 transgene and the Cre recombinase, which will induce the expression of MAGEA1 by excision of the *STOP* cassette. It should be possible to target specific tissues for MAGEA1 expression. Indeed, various transgenic mice expressing the Cre recombinase in tissues can be used, inducing a specific expression of MAGEA1.

(A)

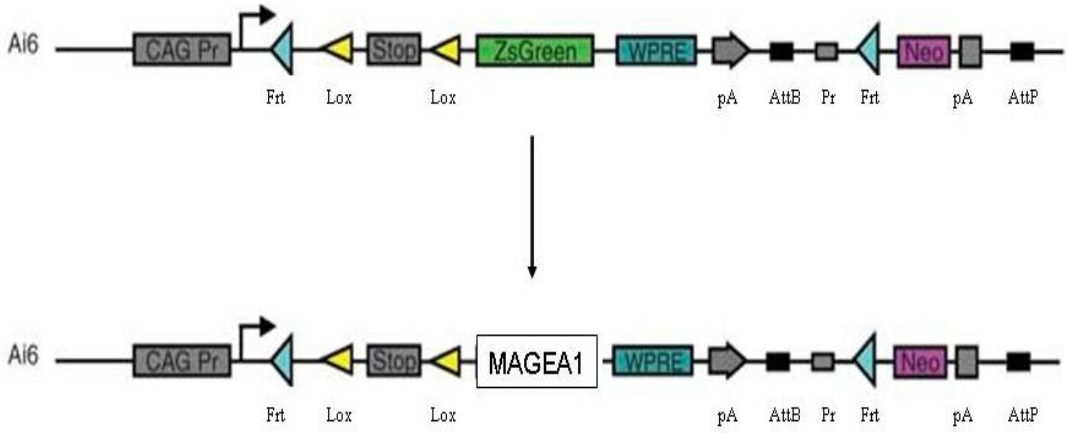

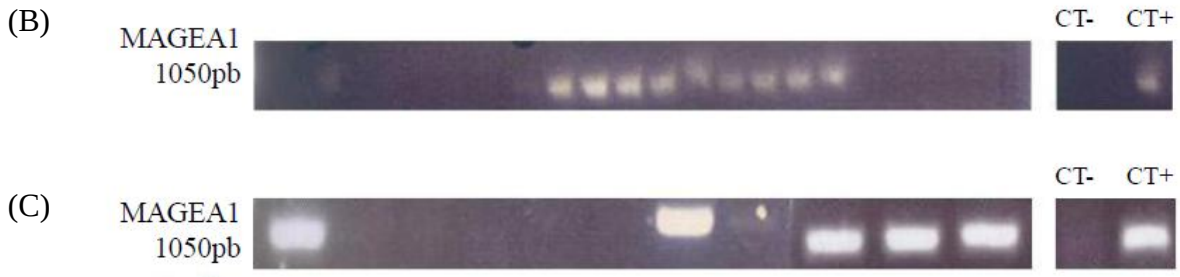

Table 2: Genotyping of Rosa26-MAGEA1 chimeric mice

	MAGEA1	**Male/Female**
Lineage n°1	1	F
Lineage n°2	1	F
Lineage n°3	1	M
Lineage n°4	2	F+M

Figure 10: (A) Plasmid map of the ai6 plasmid, in which MAGEA1 insert was cloned. CAG Pr: strong and ubiquitous promoter; Stop: floxed stop cassette; Blue triangle: Frt sites recognized by Flp recombinase; Yellow triangle: Lox sites recognized by Cre recombinase; ZsGreen: fluorescent protein; WPRE: woodshuck hepatitis virus post-transcriptional regulatory element; AttB/AttP: PGQ-Neo-marker; Neo: resistance gene to neomycin/geneticin. The ai6 plasmid is flanked by homolog sequence of the chromosome Rosa26 to allow recombination in the genome of the mice (Figure adapted from Madisen *et al*, 2010) (B) PCR genotyping of DNA extracted from tail mice (mice 0 to 41). Positive control corresponds to a TYRP-MAGEA1 positive mouse while distilled water replaces DNA for the negative control (C) PCR genotyping of DNA extracted from tail mice (mice 0 to 13). Positive control corresponds in a TYRP-MAGEA1 positive mouse while distilled water replaces DNA for the negative control. Genotyped mice correspond to brown mice, except mice 3-4-5 from founder 1, which are black mice (as second negative controls).

IN VITRO MODELS

I. MAGEA1 AND CELL CHEMORESISTANCE

1) CHEMORESISTANCE IN A P53 WILD-TYPE CELL MODEL

In addition to the projects with the MAGEA1 transgenic mice, our lab also aimed to study the involvement of MAGEA1 in chemoresistance through *in vitro* cell models (Figure 5). For this purpose, two cell models were generated: the first was a mammary epithelial cell line untransformed but spontaneously immortalized: the MCF-10A cell line. The second model was a transformed immortalized epithelial mammary cell line: MCF-7 cells. Both MCF-10A and MCF-7 cells were transducted by a lentiviral vector containing MAGEA1 under control of the PGK (phosphoglycerate kinase) promoter (or empty lentiviral vector, as control). Cells were selected with neomycin. The MCF-10A^{CT} (control) and MCF-10A ^{MAGEA1} (expressing MAGEA1) cells as well as MCF-7^{CT} and MCF-7^{MAGEA1} cells were used in chemoresistance assays.

The expression of MAGEA1 in transduced MCF-7 and MCF-10A cells was monitored by western-blotting (Figure 11). Additionally, the p53 protein level was assessed in order to evaluate the repression of p53 by MAGEA1 in our cell model. In this purpose, proteins were collected 30 minutes or 1 hour after treatment with etoposide (or without treatment, as control). Indeed, the stabilization of p53 protein requires a cellular stress, as a treatment with a DNA damaging agent such as etoposide. Figure 11A revealed a lower level of the p53 protein in presence of MAGEA1 1 hour after the treatment with etoposide in MCF-10A cells. Figure 11B shows a diminution of p53 levels in MCF-7 cells 1 hour post-treatment. These results are in accordance with the known role of MAGEA1 in the degradation of p53.

(A) (B)

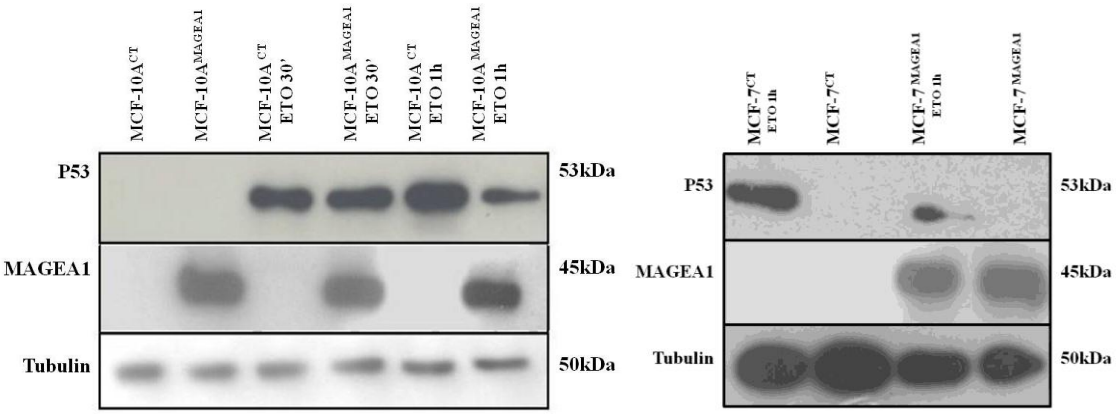

Figure 11: Western-blot analysis of proteins from (A) MCF-10A and (B) MCF-7 cells transducted by lentiviral vectors containing or not MAGEA1 (MCF-10A ^{MAGEA1} or MCF-10A^{CT} and MCF-7 ^{MAGEA1} or MCF-7^{CT}) and treated (ETO) or not (NT for no treatment) with etoposide. α-Tubulin was used as loading control.

After validation of our cell models, MCF-10A and MCF-7 cells were used to analyze the effect of MAGEA1 on chemoresistance upon treatment with 3 chemotherapeutic drugs: docetaxel, 5 fluorouracil and etoposide. Chemotherapeutic agents concentrations inducing 50% of MCF-10A cell death (IC50) were evaluated at 50 µM for etoposide, 15 nM for docetaxel and 100 µM for 5-FU. Regarding MCF-7 cells, IC50 were estimated at 60 µM for etoposide, 20 nM for docetaxel and 100 µM for 5-FU. MCF-10A and MCF-7 cells expressing or not MAGEA1 were cultivated in presence of chemotherapeutic drugs to monitor cell survival after treatment. Cell survival was measured through MTT tests at 0 (untreated cells), 24, 48 and 72 hours post-treatment. The results shown in Figure 12 suggested an improved cell survival in presence of MAGEA1, whatever the chemotherapeutic treatment and the cell line. Moreover, the difference of survival percentage of MAGEA1 positive cells compared to control cells increases with the duration of the treatment.

Concerning MCF-10A cells, survival of MCF-10A^{CT} and MCF-10A^{MAGEA1} became significantly different 24 hours after etoposide treatment and highly significant after 48 hours (Figure 12A). MCF-10A^{MAGEA1} resisted better than the controls to 5-FU treatment 48 hours after the treatment (Figure 12B). Finally, MCF-10A cells appeared to be less sensitive to docetaxel, showing a slower decrease in survival curves. Survival ratio differences between MCF-10A^{CT} and MCF-10A^{MAGEA1} were significant after 48 hours (Figure 12C).

In parallel, Figure 12D revealed that the difference of survival percentage between MCF-7^{MAGEA1} and MCF-7^{CT} becomes significant 48 hours after etoposide treatment and highly significant after 72 hours. After 5-FU treatment, the survival percentage of MCF-7 ^{MAGEA1} is significantly higher than the control during all treatment duration, with maintenance at 41% at 72 hours (Figure 12E). Finally, the treatment with docetaxel (Figure 12F) induces a higher survival rate of MCF-7^{MAGEA1} extremely significant at 48hours and significant at 72 hours compared to control cells. To summarize, these results hinted the hypothesis that MAGEA1 confer a resistance to apoptosis in two different cell models after various chemotherapeutic treatment.

(A)

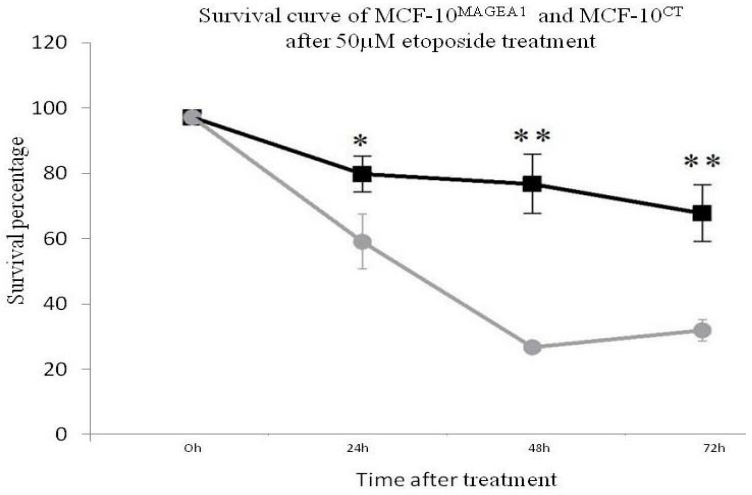
Survival curve of MCF-10MAGEA1 and MCF-10CT
after 50μM etoposide treatment
Survival percentage
120
100
80
60
40
20
0
*
**
**
0h
24h
48h
72h
Time after treatment

(B)

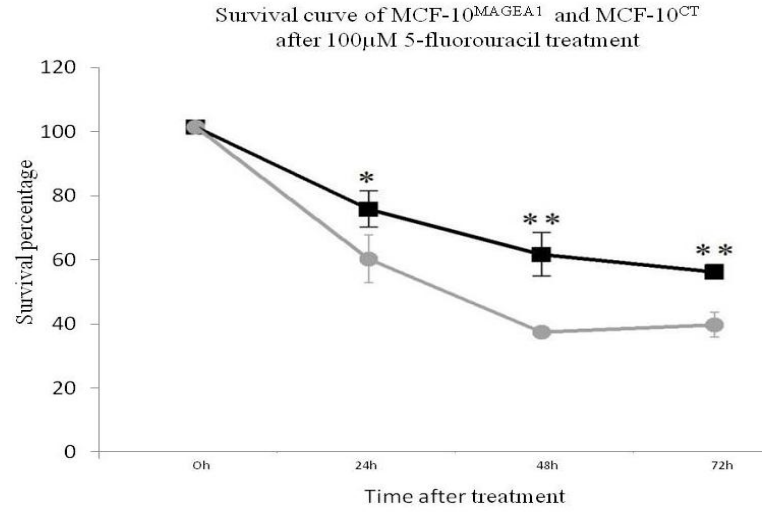
Survival curve of MCF-10MAGEA1 and MCF-10CT
after 100μM 5-fluorouracil treatment
Survival percentage
120
100
80
60
40
20
0
*
**
**
0h
24h
48h
72h
Time after treatment

(C)

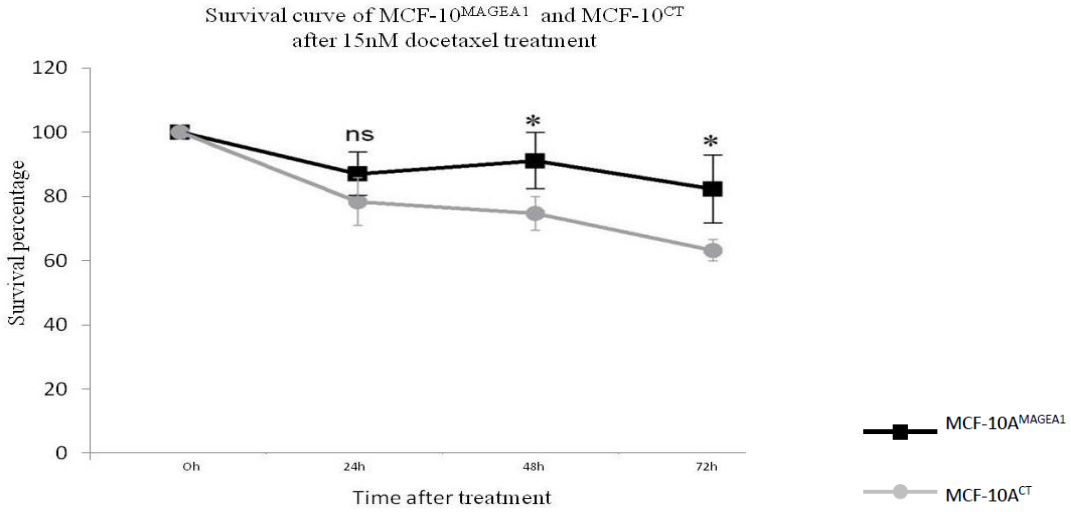
Survival curve of MCF-10MAGEA1 and MCF-10CT
after 15nM docetaxel treatment
Survival percentage
120
100
80
60
40
20
0
ns
*
*
0h
24h
48h
72h
Time after treatment
MCF-10AMAGEA1
MCF-10ACT

(D)

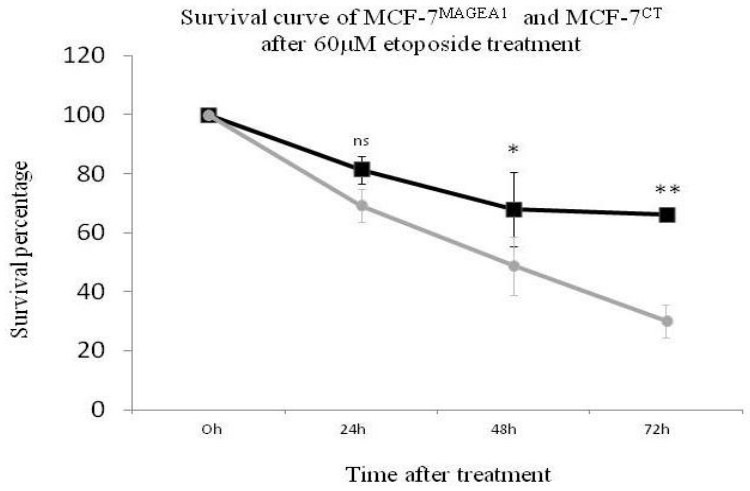
Survival curve of MCF-7MAGEA1 and MCF-7CT
after 60µM etoposide treatment
Survival percentage
120
100
80
60
40
20
0
ns
*
**
0h
24h
48h
72h
Time after treatment

(E)

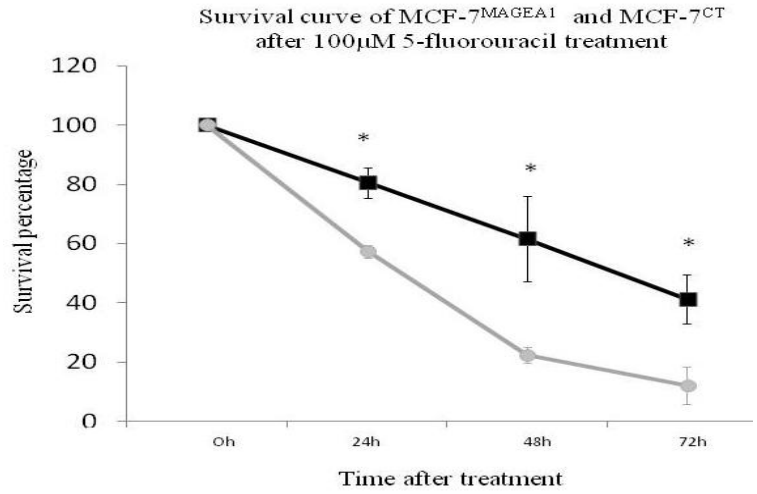
Survival curve of MCF-7MAGEA1 and MCF-7CT
after 100µM 5-fluorouracil treatment
Survival percentage
120
100
80
60
40
20
0
*
*
*
0h
24h
48h
72h
Time after treatment

(F)

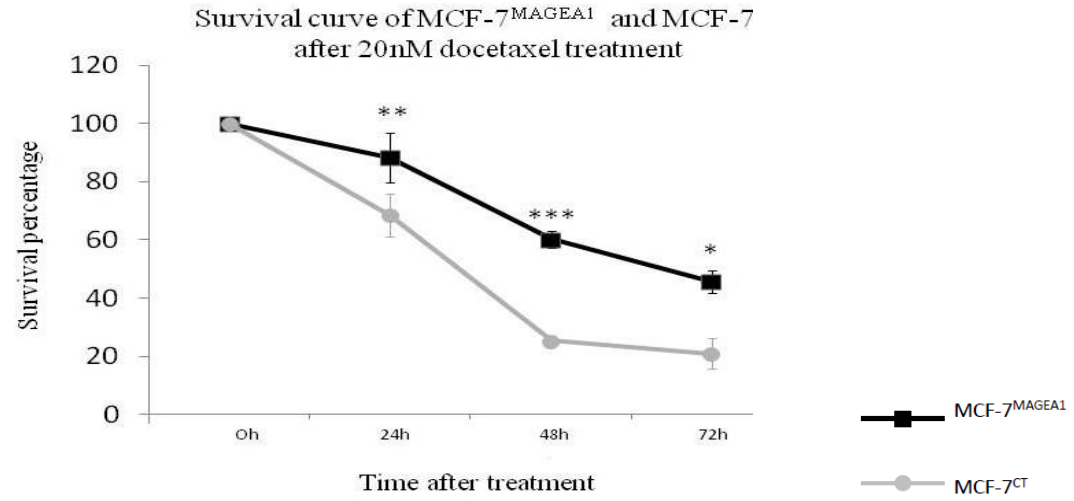
Survival curve of MCF-7MAGEA1 and MCF-7
after 20nM docetaxel treatment
Survival percentage
120
100
80
60
40
20
0
**
***
*
0h
24h
48h
72h
Time after treatment
MCF-7MAGEA1
MCF-7CT

Figure 12: Survival curves of MCF-10A^{MAGEA1} and MCF-10A^{CT} cells after 0, 24, 48 and 72 hours of treatment with (A) 50 µM etoposide, (B) 15 nM docetaxel and (C) 100 µM 5-fluorouacil. Survival curves of MCF-7 ^{MAGEA1} and MCF-^{7CT} after 0, 24, 48 and 72hours of treatment with (D) 60 µM etoposide, (E) 20 nM docetaxel and (F) 100 µM 5-fluorouacil. Error bars correspond to standard deviation for n=3. Student test was used to determine if survival percentages differences between MCF-10A ^{MAGEA1}/ MCF-7 ^{MAGEA1} and MCF-10A ^{MAGEA1} / MCF-7 ^{CT} were extremely significant (***), highly significant (**) significant (*) or non-significant (ns).

2) CHEMORESISTANCE IN A P53 DEFICIENT CELL MODEL

Our next purpose was to determine if MAGEA1 could confer chemoresistance independently of p53. It is known that cell death induced by etoposide and 5-FU is dependant of the p53 pathway. Etoposide stabilizes double strand breaks after inhibition of the topoisomerase II. The maintenance of DNA breaks leads to the activation of the kinase ATM (*ataxia telangiectasia mutated*), a serine/threonine kinase. ATM binds and neutralizes MDM2, an ubiquitine ligase responsible for p53 degradation. In this manner, the p53 protein is stabilized, leading to a p53-dependent apoptosis (Heisig *et al*, 2009).

In the same way, 5-FU is also reported to work through a p53-dependent way. 5-FU, an analog of pyrimidin, is incorporated in DNA then excised by a nucleotide repair complex. This reaction creates single strand DNA breaks, stimulating the kinase ATM and the apoptosis dependent of p53 (Grem et al. 2001; Cheng et al. 2012). Both etoposide and 5-FU thus induce p53 activation through genotoxic stress, inducing transcription of genes involved in cell cycle arrest and apoptosis (Meley *et al.*, 2010; Sun *et al.*, 2007). Consequently, chemoresistance conferred by MAGEA1 to etoposide and 5-FU could be due to its anti-p53 activity.

In contrast, the mode of action of docetaxel is described to be independent of p53. (Mhaidat NM *et al.*, 2007 a; b). Docetaxel is an anti-mitotic agent causing the stabilization of the β-tubulin, the blockage of the mitotic spindle and cell apoptosis. It has been demonstrated that p53 inhibitors do not confer chemoresistance to docetaxel, suggesting a p53-independent mechanism (Mhaidat et al. 2007). These observations raised a new question: Could MAGEA1 confer a p53-independent chemoresistance? With the aim to answer this question, we set up a p53-independent cell model by forcing expression of MAGEA1 in Hep3B cells, which are deficient for p53 and do not express type I MAGE genes. Western-blot assay validated that Hep3B cells do not express MAGEA1 or other MAGE proteins that can be recognized by the MAGEA1 antibody (Figure 13A). Expression of MAGEA1 in Hep3B cells was induced by transduction as described above (*see details in Materials and Methods*). Western-blot analysis was then performed to verify the expression of MAGEA1 in the Hep3B^{MAGEA1} cell line (Figure 13B).

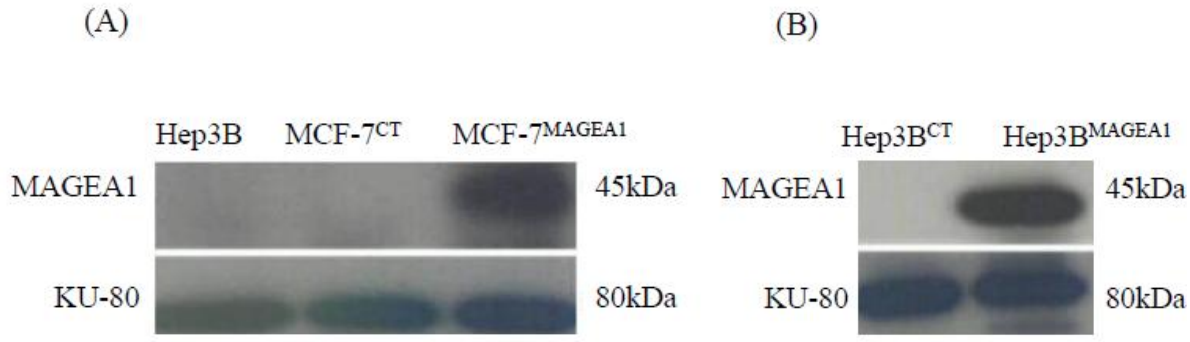

Figure 13: (A) Western-blot analysis of proteins extracted from Hep3B cells and MCF-7 cells stably expressing MAGEA1 gene (MCF-7^{MAGEA1}) or not (MCF-7^{CT}) as positive or negative control, respectively. KU-80 was used as loading control. (B) Western-blot analysis of proteins extracted from Hep3B cells, previously transducted by the lentiviral vector containing MAGEA1 (Hep3B^{MAGEA1}) or by the empty (Hep3B^{CT}) vector.

Chemoresistance was examined after treatment with DNA damaging agent, just as performed on MCF-10A and MCF-7 cells. Results shown in Figure 14A and 14B do not reveal any resistance of Hep3B^{MAGEA1} cells after etoposide and 5-FU treatments. Indeed, the differences between survival of Hep3B^{MAGEA1} and Hep3B^{CT} cells treated with etoposide or 5-FU were not significant. These observations indicate that MAGEA1 does not confer chemoresistance to Hep3B$^{p53-/-}$ cells after etoposide and 5-FU treatment.

In contrast, Figure 14C revealed a significant difference in the survival percentage between Hep3B^{MAGEA1} and control cells 48 hours after docetaxel treatment. This difference becomes highly significant after 72 hours post-treatment with a survival percentage maintained at 63% in presence of MAGEA1, in comparison with 43% in control cells. These results suggest that MAGEA1 is able to confer chemoresistance to Hep3B$^{p53-/-}$ after docetaxel treatment, reported to work independently of the p53 pathway. In other words, MAGEA1 could confer chemoresistance by a p53-independent mechanism.

(A)

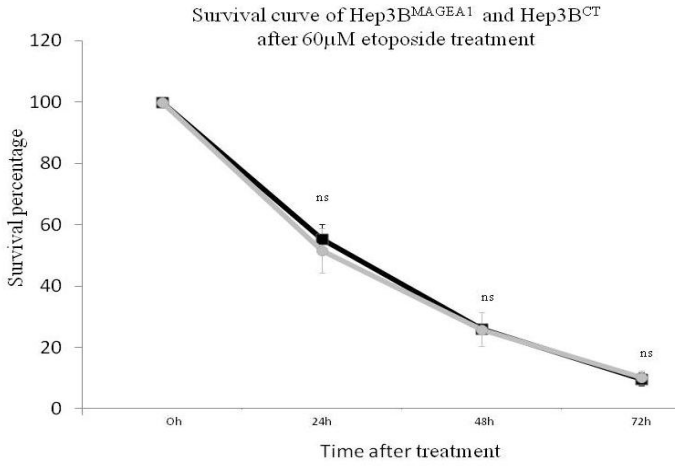

(B)

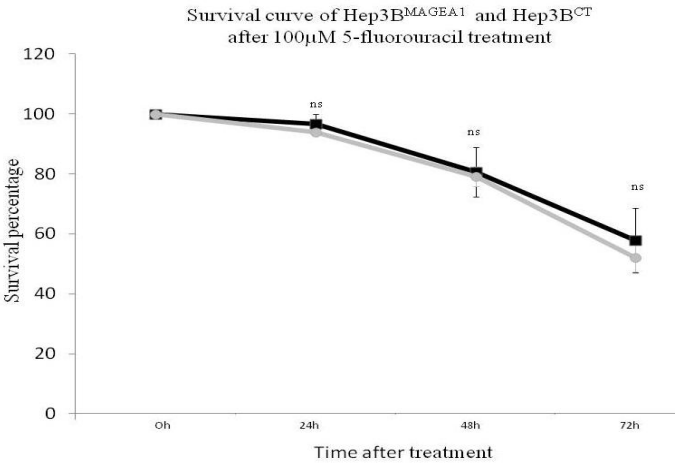

(C)

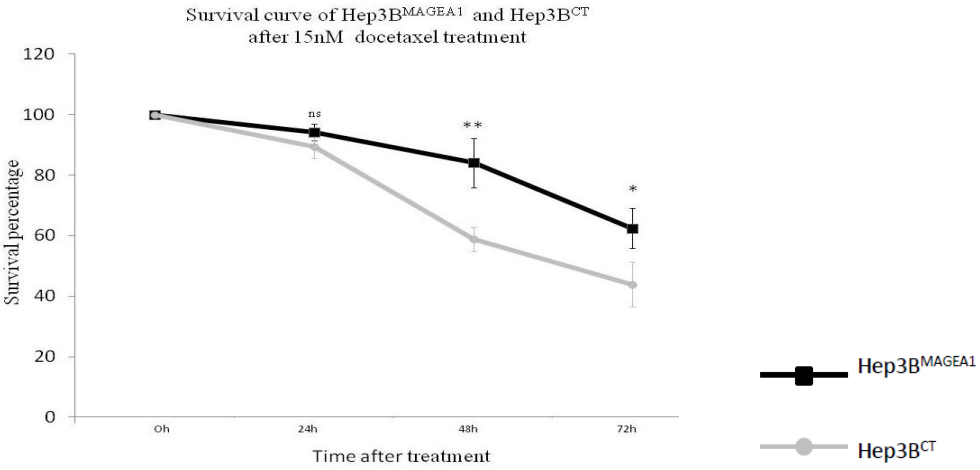

Figure 14: Survival percentage of Hep3B^{MAGEA1} and Hep3B^{CT} after 0, 24, 48 and 72hours of treatment with (A) 50 µM etoposide, (B) 100 µM 5-fluorouacil and (C) 15 nM docetaxel. Error bars correspond to standard deviation for n=3. Student test was used to determine if survival ratio differences between MCF-10A^{MAGEA1} and MCF-10A^{CT} were, significant (*) or highly significant (**) or no-significant (ns).

II. MAGEA1 AND ABC TRANSPORTERS EXPRESSION

Our next goal was to identify the p53-independent pathway responsible for the chemoresistance conferred by MAGEA1 after docetaxel treatment (Figure 5). As they are an important mediators of multidrug resistance, we investigated the effect of MAGEA1 on the expression of ATP-Binding Cassette (ABC) genes specifically on ABC-B, -C and –G families, that are known to confer multi-drug resistance.

1) ABC transporters expression in a p53 wild-type cell model

MCF-10A^{MAGEA1} cells were used to quantify the levels of several ABCs transcripts by quantitative RT-PCR in a p53 wild-type cell model (Figure 15). The choice of ABCs transporters (namely ABC- G2, -C1, -C2, -C3, -C4 and –C5) was done according to their susceptibility to be expressed in the mammary epithelium and thus in MCF-10A cells. Results show an up-regulation of ABCs transporters in presence of MAGEA1 (Figure 15). Specifically, ABCG2 gene presents a strong over-expression of 23, 7% in MCF-10A^{MAGEA1} cell compared to control cells. The ABCC1, ABCC2, ABCC4 and ABCC5 genes are less up-regulated, with a mRNA relative expression of 4,7%, 7%, 7,5% and 8,9%, respectively. A possible explanation is that the up-regulation of ABC transporters could participate to the resistance to apoptosis of MCF10A ^{MAGEA1} after etoposide treatment.

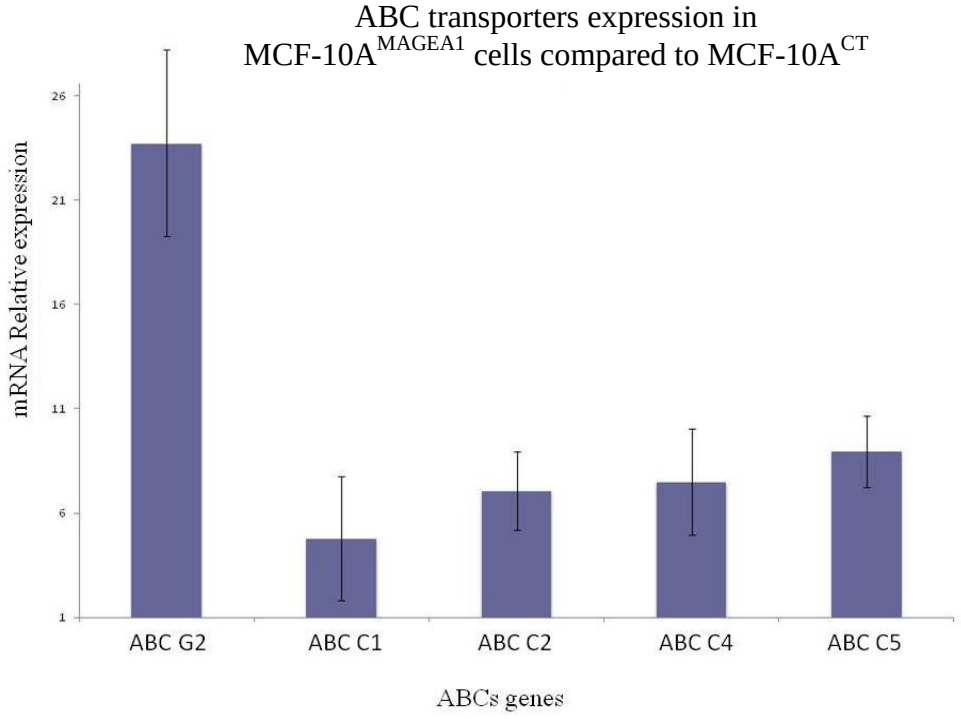

Figure 15: Quantitative PCR analysis following reverse transcription. Relative expression of ABCs genes in MCF-10A cells expressing MAGEA1 compared to control cells (MCF-10A^{CT}) 48 hours after etoposide treatment. The expression in control cells is considered as reference = 1. Error bars correspond in standard deviation for n=3.

2) ABC transporters expression in a p53-deficient cell model

In order to assess the possible role of p53 in the induction of ABCs, we repeated the experiment in the p53-deficient Hep3B cells. ABC-C1, -C2, -C4, -C5, -B1 and –B11 were selected for their specificity for the hepatic tissue. Results indicated in Figure 16 do not reveal any up-regulation of ABC transporters in Hep3B^{MAGEA1} compared to control cells (Hep3B^{CT}).

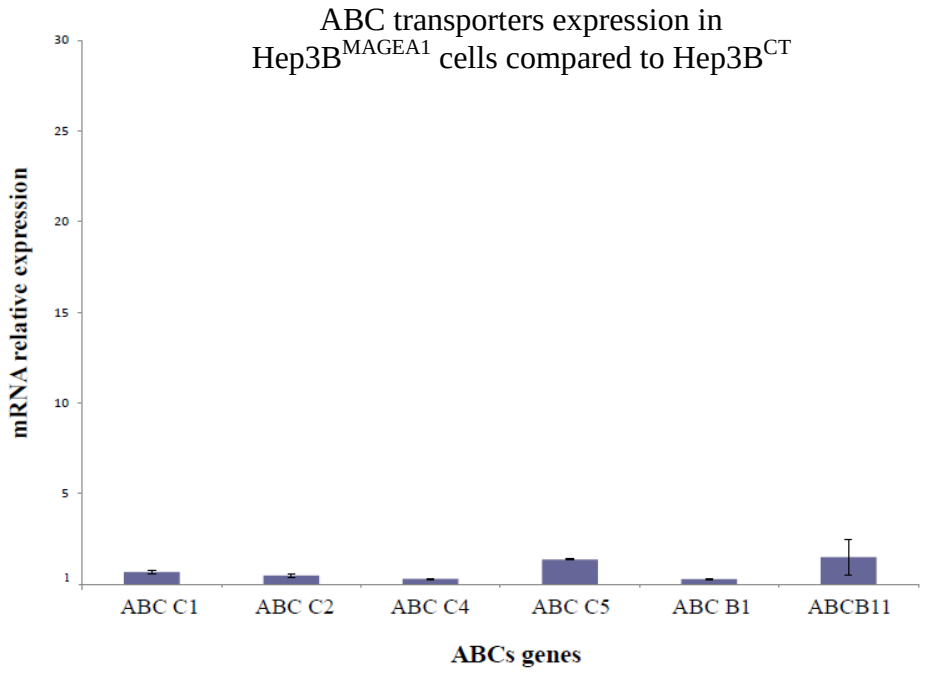

Figure 16: Quantitative PCR analysis following reverse transcription. Relative expression of ABCs genes in Hep3B cells expressing MAGEA1 compared to control cells 48 hours after etoposide treatment. The expression in control cells is considered as reference = 1. Error bars correspond to standard deviation for n=3.

These results show that ABCs transporters, often involved in multi-drug resistance are induced by MAGEA1 in MCF-10A cells, but not in Hep3B. A possible explanation is that the induction of ABCs transporters could be dependent of the p53 pathway. This hypothesis is supported by a study published in 1997 which demonstrate that p53 was able to repress the transcription of ABC transporters by direct binding to their promoter regions (Thottassery et al., 1997). However, no conclusions can be made at this time, as the experiment was performed with two different cell models. To confirm this hypothesis, we need to compare identical cells except for the expression of p53.

III. MAGEA1 AND CELL MIGRATION

1) EFFECT OF MAGEEA1 ON MIGRATION IN A P53 WILD-TYPE CELL MODEL

In order to explore other oncogenic properties of MAGEA1, the role of MAGEA1 in cell migration and invasion was assessed in the lab (Figure 5) (Elise Srour, unpublished data). Cell migration is a crucial step for tumor development, as it allows cancer cells to invade the surrounding tissues. Additionally, Jung and his team had proved an association between MAGEA genes and development of metastasis, but no *in vitro* evidences of a role for MAGEA1 in cell migration was described (Jung *et al*., 2005).

We performed scratch tests on MCF-10A cells, expressing or not MAGEA1. The principle of scratch tests is to create a wound in a cell monolayer in order to measure the speed of cell migration. Figure 17 shows the pictures of MCF-10A^{CT} or MCF-10A^{MAGEA1} at different times after the scratch. The Figure 19A shows the opening percentage of the wound at different time after the scratch. Twelve hours after the scratch, MCF-10A^{MAGEA1} cells had partially closed the wound and the difference of migration between MCF-10A ^{MAGEA1} and control cells became significant. At 16 hours, MAGEA1 positive cells had totally closed the scratch, showing a difference highly significant compared to control cells. Control cells required twenty-four hours to completely close the wound. These results suggest an ability of MAGEA1 to stimulate the migration of MCF-10A cells.

2) EFFECT OF MAGEA1 ON MIGRATION IN A P53-DEFICIENT CELL MODEL

Subsequently, we aimed to study the effect of MAGEA1 in the p53 deficient cell model (Hep3B). Scratch tests were performed on Hep3B^{MAGEA1} and Hep3B^{CT} cells, both deficient in p53. Figure 18 presents the pictures taken at different intervals after the wound while Figure 19B displays quantitative results of the assay. Whatever the interval, Hep3B cells show a similar pattern of migration independently of MAGEA1 expression. After 72 hours, the scratch was nearly closed in the two cell lineages. These scratch tests do not reveal any effect of MAGEA1 on migration in Hep3B cells.

These observations suggest that MAGEA1 is able to confer a migratory advantage to MCF-10A cells, but not to Hep3B, deficient for p53. It would be interesting to perform this experimentation of MCF-10A cells knock-out for p53 to confirm the role of p53 in this process. This hypothesis is in accordance with the well-known role of the p53 pathway in cell migration (Roger *et al*, 2006). Beside its involvement in cell cycle progression and apoptosis, p53 is also involved in the migratory characteristics of tumor cells.

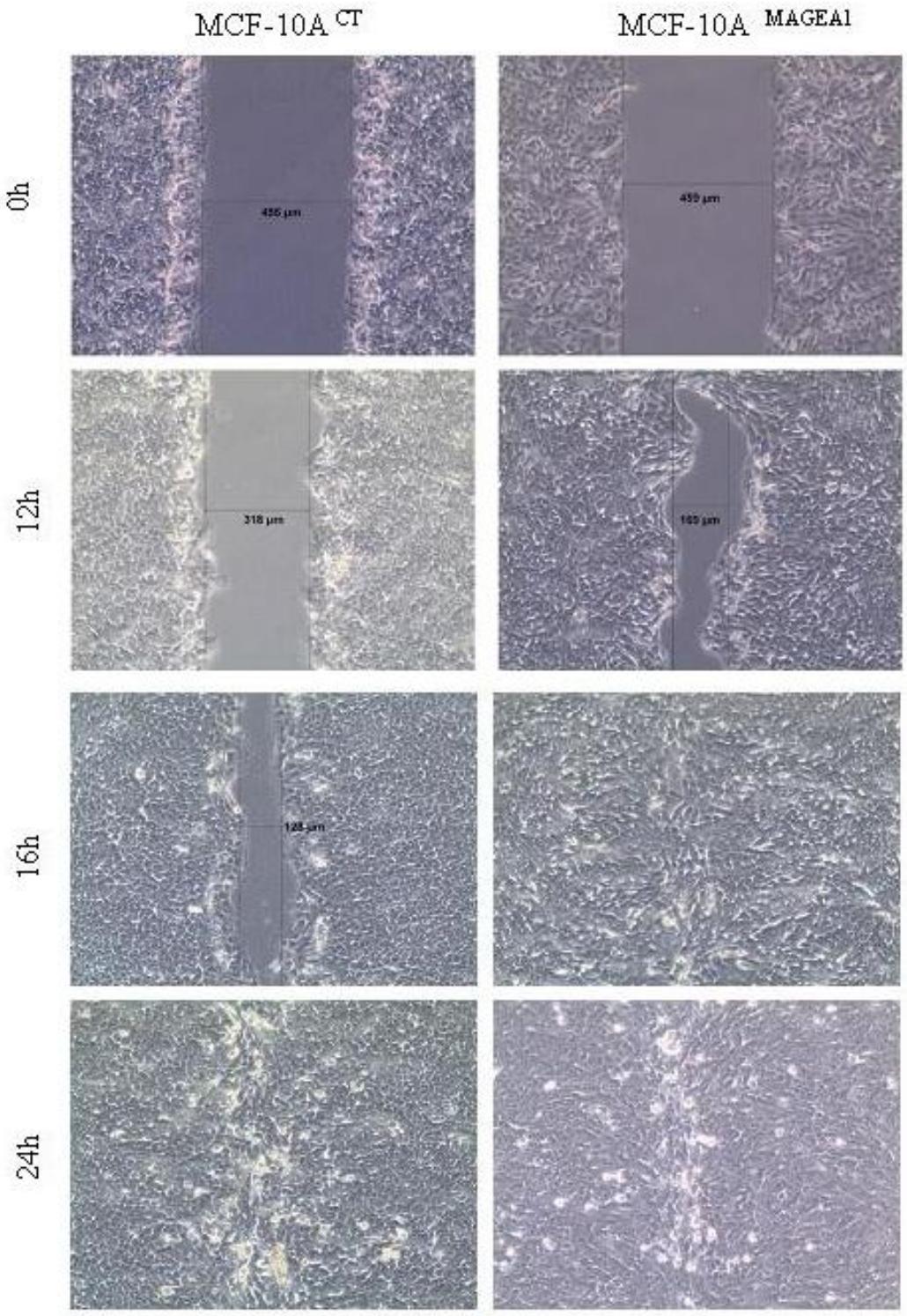

Figure 17: Pictures of the scratch test of MCF-10A cells expressing or not MAGE-A1 (MCF-10A ^{CT} and MCF-10A ^{MAGEA1}). Pictures were taken 0h, 12h, 16h and 24h after the scratch. For each interval, scratch tests were performed three times at three different positions. The average distance between the two cell walls was measured using the software PhotoFiltre 7.

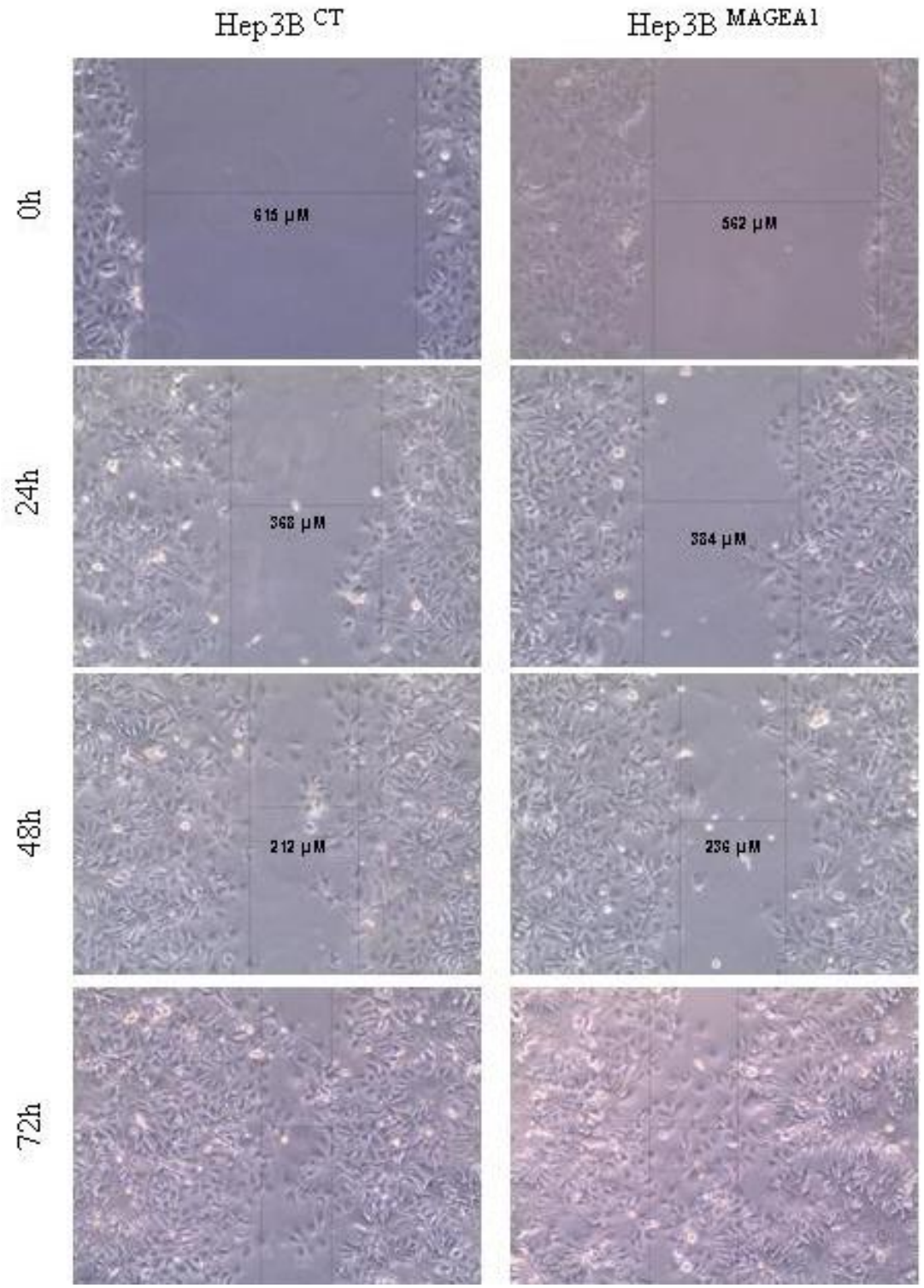

Figure 18: Pictures of the scratch test of Hep3B cells expressing or not MAGE-A1 (Hep3B ^{CT} and Hep3B ^{MAGEA1}). Pictures were taken 0h, 24h, 48h and 72h after the scratch. For each interval, scratch tests were performed three times at three different positions. The average distance between the two cell walls was measured using the software PhotoFiltre 7.

(A)

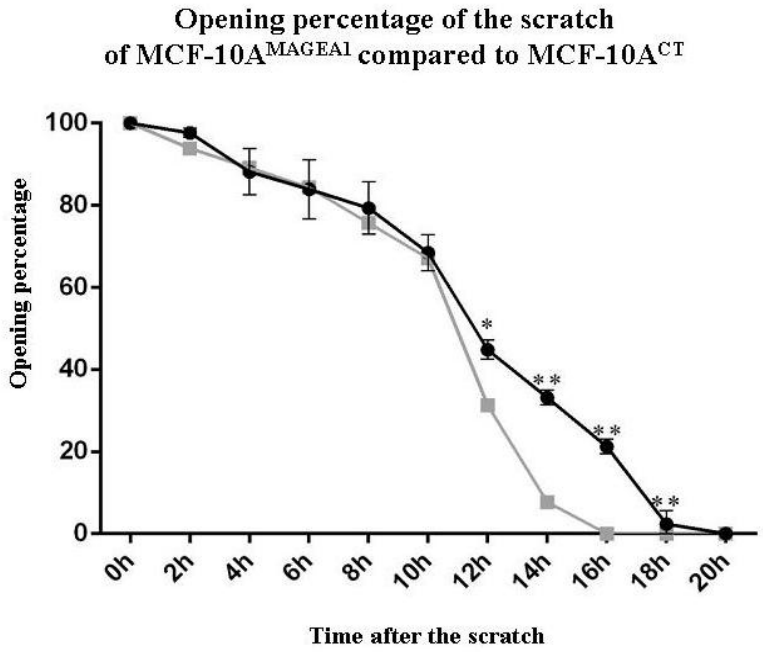

(B)

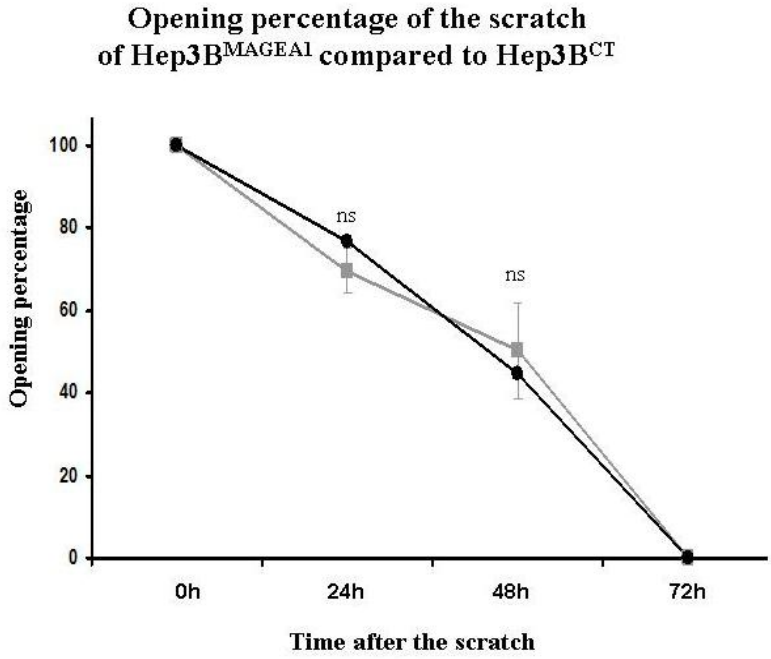

Figure 19: Quantification of scratch tests by measuring the opening percentage of the scratch (A) on MCF-10A^{MAGEA1} and MCF-10A^{CT} and (B) on Hep3B^{MAGEA1} and Hep3B^{CT}. Errors bars represent standard deviation for n=3 for (A) and n=2 for (B). Student test was used to determine if survival percentages differences between MCF-10A ^{MAGEA1}/ Hep3B ^{MAGEA1} and MCF-10A ^{MAGEA1} / Hep3B ^{CT} were extremely significant (***), highly significant (**) significant (*) or no-significant (ns).

DISCUSSION

IN VIVO MODELS

One objective of my project was to generate and start to characterize transgenic mice ectopically expressing MAGEA1 in melanocytes. The expression of MAGEA1 was quantified in four different mice lineages and different organs (skin, liver, heart, brain and testis). Brain and testis were chosen because of their general high susceptibility to express transgenes. Quantitative RT-PCR analysis revealed a transcription of MAGEA1 in the skin of each mouse lineage. This observation is in accordance with the expected results. Indeed, the specificity of MAGEA1 transcripts in the skin was predictable, as a promoter derived from the tyrosinase gene was used to drive the expression of MAGEA1. Note that the tyrosinase is an enzyme needed for melanin production and specifically expressed in melanocytes. Melanocytes are also present in non-cutaneous tissues, such as in the retina of the eye, gastro-intestinal and genito-urinary mucosa and brain, specifically in meninges (Chudnovsky *et al*, 2005). However, MAGEA1 transcripts were undetectable in the brain of the transgenic mice. For this reason, analyses of other organs (containing non-cutaneous melanocytes for example) are required.

The difference of MAGEA1 expression level among the different lineages could be explained by the transgene copy number. Indeed, additive transgenesis is known to generate mice with multiple transgene copies inserted in the genome in a single or multiple loci. In addition, the locus of insertion could also affect the expression of the transgene. The advantage of this phenomenon is the possibility to compare the effect of MAGEA1 according to its level of expression in different mouse lineages.Another objective of the work was to confirm the expression of MAGEA1 at a protein level in transgenic mice, through western-blotting using the 6C1 anti-MAGE antibody. The analysis revealed a band of approximately 45kDa but was interpreted as aspecific, given that the band was also detected in the negative control. The CleanBlot secondary antibody allowed the elimination of the interference with the immunoglobulin heavy chains. The blot did not reveal any band, except in the positive control, suggesting that the protein previously detected corresponded to the immunoglobulins present in mouse tissues. Actually, this result could be expected since the 6C1 MAGEA antibody is a murine monoclonal antibody with a mouse constant domain. No MAGEA1 protein was identified in the skin of the transgenic mice. One possible explanation is that the level of MAGEA1 expression is too low to be detected by western-blot analysis. MAGEA1 is supposed to be exclusively expressed in melanocytes, which only constitute a very small proportion of epidermal cells. The isolation of skin melanocytes could be performed by FACS sorting, for instance by crossing the TYRP-MAGEA1 transgenic mice with TYRP-GFP mice. Another method is to analyze MAGEA1 expression by immunohistochemistry using a rabbit MAGEA1 antibody. This experiment is ongoing. The lab also generated MAGEA1 transgenic mice by targeted transgenesis, in parallel to the transgenic mice obtained by direct transgenesis. The inducible mouse model Rosa26-MAGEA1 presents an important advantage. Indeed, these mice could be crossed with different Cre expressing mice (ubiquitous, inducible or specifically in a certain tissue) to force the expression of MAGEA1 in different tissues to evaluate tumor development.

The long term goal of this *in vivo* project is to determine if MAGEA1 enhances tumor development, chemoresistance or metastasis. In TYRP-MAGEA1 mice, the specific development of melanomas will be monitored. The choice of melanocytes was motivated by the fact that MAGEA1 is predominantly expressed in melanoma. Moreover, skin tumors are easily detected by observation of the mice. We aim to induce tumor development in these mice using different ways:

One way consist in treating the mice with DMBA/TPA (7,12 dimethyl benz(a)anthracene / 12-O-tetradecanoylphorbol-13-acetate) (Indra *et al*, 2007). DMBA is a powerful carcinogen able to initiate melanoma. Just a single topical application induces the initiation stage. Following that, tumor growth can be provoked by TPA, a tumor promoter which enhances a continuous hyperplasia and inflammation, which will lead to melanomas (Indra *et al*, 2007; Yuspa *et al*, 1998). But the main obstacle of this experimentation is the experimenter biosafety.

Another possible method to induce melanomas is to mate the MAGEA1 transgenic mice with mice spontaneously developing melanomas. The transgenic mice $Ink4a^{-/-}/Arf^{-/-}/Ras^{+/+}$ is reported to be an appropriate model for melanoma development (Figure 20).

The INK4A (or $p16^{INK4A}$) and ARF (or $p14^{ARF}$) are tumor suppressor proteins encoded by the CDKN2A locus, present on the 9p21 chromosome. An alternative promoter allows the specific splicing of CDKN2A in two spliced isoforms: INK4A and ARF. INK4A and ARF, present a different first exon (1α and 1β, respectively) and common second and third exons but in alternating reading frames (Chin *et a*l, 2003; Chudnovsky *et al* 2005). INKA4, a member of the INK4 (inhibitor of cyclin-dependent kinase 4) family, is able to bind and inhibit the cyclin-dependent kinases Cdk4 and Cdk6. The kinases Cdk4 and Cdk6 inactivate the retinoblastoma protein (Rb) by phosphorylation, allowing the advancement of the cell cycle to the S phase (Serrano *et al*, 1993; Serrano *et al*, 1996). This way, INK4A loss leads to Rb inactivation and uncontrolled cell cycle. In other part, ARF permit the stabilization of the p53 tumor suppressor by inhibition of MDM2, responsible for the degradation of p53 in a proteasome-dependent manner. In consequence, the loss of ARF induces the degradation of p53 (Zhang et al, 2003). Interestingly, 25% to 40% of the familial melanomas present a mutation in INK4A/ARF (Aitken et al, 1999, Tsao et al, 2000). Furthermore, mice knock-out for the INK4A gene have a higher susceptibility to develop melanomas (Krimpenfort *et al*, 2001). All together, these observations suggest that the pathway INK4A/ARF is a prominent suppressor axis in human melanoma. Moreover, Chin and his team detect a synergism between the activation of the Ras pathway and the combined loss of INK4A/ARF in melanoma development in mice. Transgenic mice expressing Ras in melanocytes develop melanomas in 43% of the cases in 6 months-period in an INK4A/ARF deficient background (Ackermann *et al*, 2005; Chin *et al*, 1997; Chin *et al*, 2003; Huijbers *et al*, 2006).

Our purpose is to mate the $Ink4a^{-/-}/Arf^{-/-}/Ras^{+/+}$ mice with the MAGEA1 transgenic mice in order to obtain a MAGEA1 transgenic mice which spontaneously develop melanomas (Figure 20). Besides, we shall monitor the size, the number and the aggressiveness of tumors in MAGEA1 mice compared to control mice ($Ink4a^{-/-}/Arf^{-/-}/Ras^{+/+}$). It will also be interesting to study the state of the p53 protein in these mice by western-blot analysis after treatment with a DNA damaging agents. Indeed, a DNA damaging agent, as a chemotherapeutic treatment, is needed to stabilize the p53 protein level. Moreover, chemoresistance of the tumors in these mice could be evaluated.

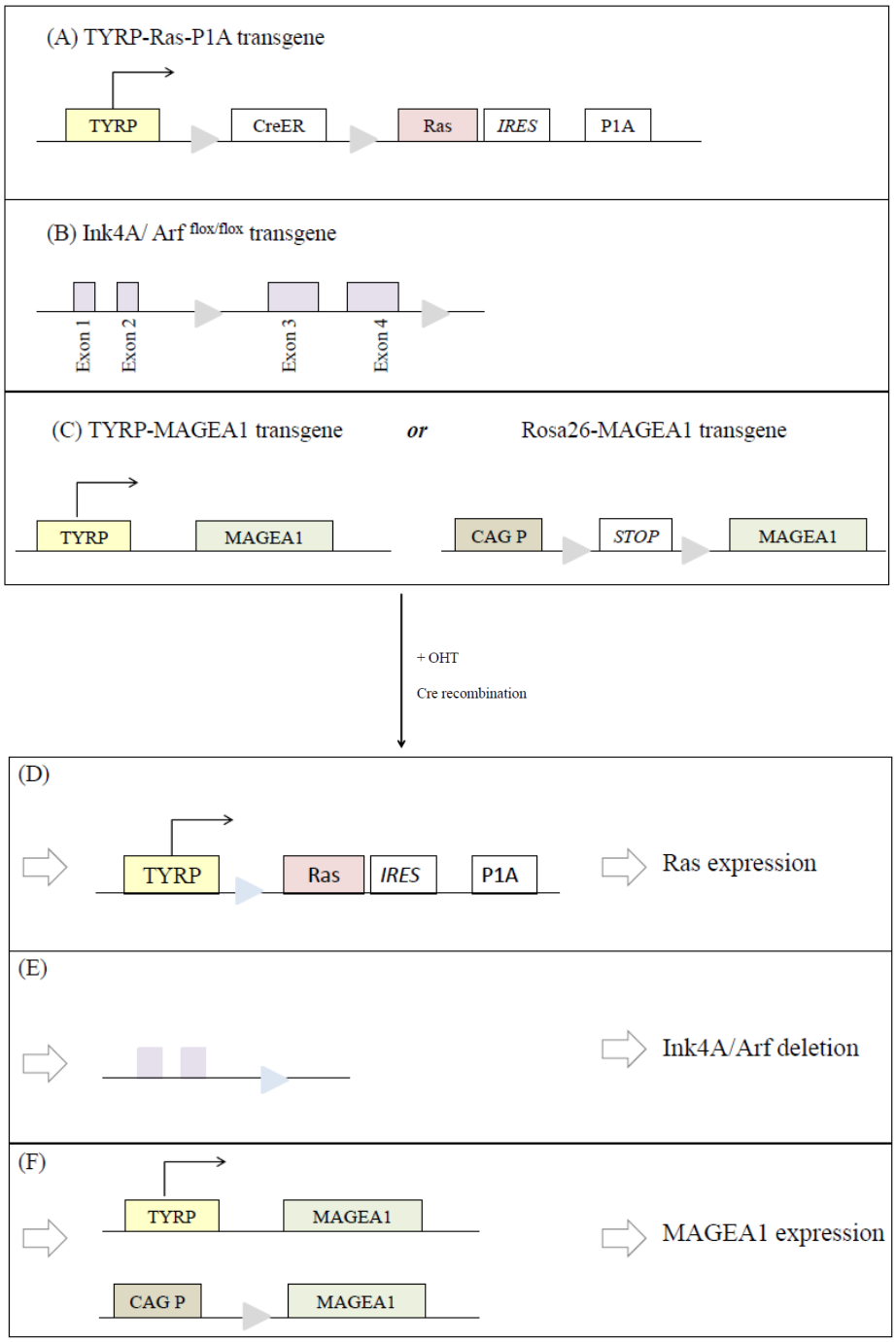

Figure 20: The Ink4a$^{-/-}$/Arf$^{-/-}$/Ras$^{+/+}$ inducible mouse model of melanoma. (A) Map of the transgene Tyr-Ras-P1A. The tyrosinase promoter is followed by a Cre-recombinase inducible with tamoxifen (or OHT for 4-OH-tamoxifen) and flanked by lox sites. The H-Ras gene expression is driven by the tyrosinase promoter to allow a specific expression of Ras in melanocytes. P1A corresponds to a surface antigen and contain the signal of poly-adenylation. The Ras transgene is introduced in mice with a homozygous conditional Ink4a/Arf locus, flanked by loxP sites (see (B)). (C) Map of the TYRP-MAGEA1 mouse and of the Rosa26-MAGEA1 mouse. Our purpose is to cross these mice with the Ink4a$^{-/-}$/Arf$^{-/-}$/Ras$^{+/+}$ mouse model. After OHT administration, the Cre-recombinase will recombine genes flanked by loxP sites, thereby inducing (D) the activation of H-Ras and P1A combined with the self-deletion of Cre, (E) the loss of Ink4a/Arf and (F) the expression of MAGEA1 in the inducible Rosa26-MAGEA1 mouse (Figure adapted from Huijbers *et al,* 2006).

An important aspect to take into account in these *in vivo* models is the use of the human MAGEA1 sequence to generate the MAGEA1 transgenic mice. There is no evidence that the functions of the MAGEA1 human protein are conserved in a mouse content. For this reason, we shall induce MAGEA1 in mouse cells and determine if MAGEA1 interferes with expression and functions of p53. For instance, we could evaluate the p53 transactivation functions by performing a luciferase reporter assay and analyzing the expression of its target genes p21, Bax and Puma by western-blot analysis.

IN VITRO MODELS

The second main goal of this project aimed to study the involvement of MAGEA1 in chemoresistance and migration using *in vitro* models. We demonstrated that MAGEA1 conferred chemoresistance to MCF-10A and MCF-7 cells after treatment with 3 chemotherapeutic drugs: etoposide, 5-FU and docetaxel, chosen for their distinctive mode of action. The chemoresistance assays were reiterated on Hep3B^{MAGEA1} and Hep3B^{CT} cells after treatment with the same chemotherapeutic drugs. The obtained results show a chemoresistance of Hep3B cells only after docetaxel treatment. Intriguingly, Etoposide and 5-FU are reported to be dependent of the p53 pathway, by stimulating the kinase ATM. On the other hand, the mode of action of docetaxel is not entirely determined. Docetaxel is an anti-mitotic able to engender the stabilization of the β-tubulin leading to the blocking of the mitotic spindle and cell apoptosis. Mhaidat *et al* hypothesized that docetaxel treatment could induce activation of caspase-2 (Mhaidat *et al*, 2007). Once activated, caspase-2 induces the translocation of Bax through the mitochondrial membrane, leading to mitochondrial apoptosis. It has been demonstrated that p53 inhibitors do not confer chemoresistance to docetaxel, suggesting a p53-independent mechanism (Mhaidat et al. 2007). These findings hint the possibility that MAGEA1 could confer chemoresistance after inhibition of caspase-2. Interestingly, it has been reported that MAGE proteins are able to bind and stimulate caspases (specifically caspase 3, 9 and 11), suggesting a possible interaction between MAGE proteins and caspases. For this reason, it could be very interesting to study the interference between MAGEA1 and caspase 2. It could be interesting to monitor the expression of caspase-2 by western-blot analysis in cells expressing or not MAGEA1 after docetaxel treatment.

Analysis by quantitative RT-PCR revealed an over-expression of several ABC transporters in MCF-10A cells after treatment with etoposide. The same experiment on Hep3B cells, deficient for p53, revealed no significant ABCs over-expression in Hep3B^{MAGEA1} compared to control cells. In order to quantify the expression of ABC in another p53 wild-type cell model, the study of ABC transporters expression in MCF-7^{MAGEA1} and MCF-7^{CT} cells is ongoing. It can also be interesting to study the ABCs expression in these cell models after treatment with 5-FU and docetaxel. In addition, it would be interesting to evaluate the activity of ABC transporters. ABCs activity can be measured by FACS analysis using a fluorescent substrate of ABCs. For instance, etoposide is naturally fluorescent and transported by ABC-G2, hoescht is a substrate for ABC-B1, -C1 and –G2 and finally the rhodamine is also reported to be recognized and transported by ABC-B1. Thereafter, activity of ABC transporters is evaluated by FACS analysis. The measure of fluorescence will allow us to determine if the ABC protein had transported the substrate into the cell. Specific inhibitors of ABC can also be used, as the fibroblast growth factor (FGF), that target ABC-B1 and induce its inhibition. This will permit to determine if chemoresistance is due to the induction of ABC transporters or not. So, we could perform chemoresistance assays with or without the inhibition of ABC transporters and compare the results.

Another purpose of my work was to study the role of MAGEA1 in cell migration. Scratch tests on MCF-10A cells expressing or not MAGEA1 were previously performed in the lab. Results revealed a faster migration of cells in presence of MAGEA1. To study the pathway involved in the acceleration of cell migration, we started the experiment again on Hep3B cells, deficient in p53, but detected no difference in cell migration. It should be interesting to make this experiment on MCF-10A cells knock-out for p53 to determine if the migration enhanced by MAGEA1 is dependent on the p53 pathway. A possible pathway involved in the acceleration of cell migration by MAGEA1 could implicate the E-cadherin protein, needed for the stabilization of the adherent junctions. Indeed, it has been previously demonstrated in our lab that the level of E-cadherin, a protein essential for maintenance of adherent junctions, was diminished in presence of MAGEA1 (Elise Srour, unpublished data). Some studies showed that the inhibition of the E-cadherin is an important contributing factor for cell migration in cancer cells (van Roy & Berx 2008).

An interesting assay to perform in these *in vitro* studies involve the generation of the same cell model for studying the p53 dependent and independent effects of MAGEA1. Indeed, the chemoresistance and migration assays should be repeated on MCF-10A cells which do not express p53, for example by using p53 targetted shRNA. If the inhibition of p53 restores the chemoresistance and migratory phenotype observed in Hep3B cells, we shall determine the p53-independent functions of MAGEA1.

The soft-agar assay is the gold standard test to assess cell transformation *in vitro*. Indeed, cell transformation is characterized by several phenotypic changes such as the ability to grow in an anchorage independent way. Previously in the lab, soft agar test on MEFs (Mouse Embryonic Fibroblast) were performed (Elise Srour, unpublished data). The MEFs were stably transducted with the following coding sequences:

- Ras
- Myc
- Ras + Myc
- MAGEA1 + Myc
- MAGEA1 + Ras
- MAGEA1

It is important to recall that, in mice, the simultaneous expression of the oncogenes Ras and Myc induces cell transformation (so corresponding to the positive control). The MEFs expressing Ras+A1 or Myc+A1 were used to determine if MAGEA1 could enhance cell transformation. No colony formations were detected in these conditions. This suggests that MAGEA1 cannot induce cell transformation. However, expression of MAGEA1 could favor transformation, when combined with Ras + Myc. For this reason, it would be interesting to repeat this experiment with MEFs $^{RAS + MYC + A1}$ to compare the number or the size of colony with the transformed MEFs $^{RAS+MYC}$. Another test is to compare tumor development in mice injected by MEFs $^{RAS + MYC + A1}$ or MEFs $^{RAS+MYC}$.

To summarize, the *in vivo* part of this project consisted to the generation of a MAGEA1 mouse model in order to determine the role of MAGEA1 in tumorigenesis; while the *in vitro* section raised the hypothesis that MAGEA1 could confer survival and migratory advantages to several cell models.

REFERENCES

Ackermann *et al,* 2005: Ackermann, J., Frutschi, M., Kaloulis, K., McKee, T., Trumpp, A., and Beermann, F: " Metastasizing melanoma formation caused by expression of activated N-RasQ61K on an INK4a-deficient background". *Cancer Res, 2005.* 65: 4005–4011

Ansbro *et al,* 2013: Megan R. Ansbro, Suneet Shukla, Suresh V. Ambudkar, Stuart H. Yuspa, Luowei Li Screening: "Compounds with a Novel High-Throughput ABCB1-Mediated Efflux Assay Identifies Drugs with Known Therapeutic Targets at Risk for Multidrug Resistance Interference" PLOS ONE 2013; 8, 4; e60334

Aprelikova *et al,* 2009: Olga Aprelikova, Silvia Pandolfi, Sean Tackett, et al. : « Melanoma Antigen-11 Inhibits the Hypoxia-Inducible Factor Prolyl Hydroxylase 2 and Activates Hypoxic Response" *Cancer Res* 2009;69:616-624

Ariel *et al,* 1991: Ariel M, McCarrey J, Cedar H.: "Methylation patterns of testis-specific genes." Proc Natl Acad Sci USA 1991;88:2317–2321

Ariel *et al,* 1994: Ariel M, Cedar H, McCarrey J. "Developmental changes in methylation of spermatogenesis-specific genes include reprogramming in the epididymis." Nat Genet 1994;7:59–63

Aitken *et al,* 1999: Aitken, J., Welch, J., Duffy, D., Milligan, A., Green, A., Martin, N., and Hayward, N.K. 1999. "CDKN2A variants in a population- based sample of Queensland families with melanoma." *J. Natl. Cancer Inst.* 91: 446–452

Barker PA and Salehi A., 2001: Barker PA and Salehi A : « The MAGE proteins: emerging roles in cell cycle progression, apoptosis, and neurogenetic disease" J Neurosci Res. 2002 Mar 15;67(6):705-12

Barrow *et al,* 2006: Catherine Barrow, Judy Browning, Duncan MacGregor, et al: "Tumor Antigen Expression in Melanoma Varies According to Antigen and Stage" *Clin Cancer Res* 2006;12:764-771

Bhutani *et al,* 2011 : Manisha Bhutani, Ashutosh Kumar Pathak, Hongli Tang, You H. Fan, DianeD. Liu, J. JackLee, Jonathan Kurie, RodolfoC. Morice, WaunKi Hong1 and Li Mao: " Frequent expression of *MAGE1* tumor antigens inbronchial epithelium of smokers without lung cancer Experimental and Therapeutic Medicine" 2011 2: 137-142

Brasseur *et al,* 1995: Brasseur F, RimoldiD, Lie´nardD, et al: "Expression of MAGE genes in primary and metastatic cutaneous melanoma." IntJCancer1995; 63:37580

Brichard *et al,* 2013: Brichard VG, Godechal Q : « MAGE-A3-specific anticancer immunotherapy in the clinical practice". Oncoimmunology. 20131;2(10):e25995

Caballero *et al,* 2010 : Caballero OL, Zhao Q, Rimoldi D, Stevenson BJ, Svobodová S, Devalle S, Röhrig UF, Pagotto A, Michielin O, Speiser D, Wolchok JD, Liu C, Pejovic T, Odunsi K, Brasseur F, Van den Eynde BJ, Old LJ, Lu X, Cebon J, Strausberg RL, Simpson AJ. : « Frequent MAGE mutations in human melanoma » PLoS One. 2010 ;5(9). pii: e12773

Caballero et Chen, 2009: Caballero, O.L. & Chen, Y.-T. : « Cancer/testis (CT) antigens: potential targets for immunotherapy. » *Cancer science*, 2009 100(11), pp.2014–21

Carrell *et al,* 2010: Douglas T. Carrell1 and Saher Sue Hammoud : « The human sperm epigenome and its potential role in embryonic development Molecular Human Reproduction," 2010; 16.1 pp. 37–47

Chen *et al,* 2009: Chen, Li, Endler, A. & Shibasaki, F., "Hypoxia and angiogenesis: regulation of hypoxia-inducible factors via novel binding factors". *Experimental & molecular medicine*, 2009; 41(12), pp.849–57

Cheng *et al,* 2012: Cheng, M. et al.: "5-Fluorouracil Nanoparticles Inhibit Hepatocellular Carcinoma via Activation of the p53 Pathway in the Orthotopic Transplant Mouse Model" *PloS one*, 2012 7(10), p.e47115

Chin *et al,* 1997: Chin L, Pomerantz J, Polsky D, et al.: "Cooperative effects of INK4a and ras in melanoma susceptibility in vivo" Genes Dev 1997;11:2822–34

Chin *et al,* 2003; Chin L.: "The genetics of malignant melanoma: lessons from mouse and man". Nat Rev Cancer 2003;3: 559–70

Chin *et al,* 2006: Lynda Chin, Levi A. Garraway and David E. Fisher: "Malignant melanoma: genetics and therapeutics in the genomic era" *Genes Dev.* 2006 20: 2149-2182

Chomez *et al,* 2001: Patrick Chomez, Olivier De Backer, Mathieu Bertrand, et al. : « An Overview of the *MAGE* Gene Family with the Identification of All Human Members of the Family" *Cancer Res* 2001;61:5544-5551.

Chudnovsky *et al,* 2005: Chudnovsky, Y., Adams, A.E., Robbins, P.B., Lin, Q., and Khavari, P.A.: "Use of human tissue to assess the oncogenic activity of melanoma-associated mutations". *Nat. Genet.2005* 37: 745–749.

Clotman, F. *et al*., 2000: Clotman F, De Backer O, De Plaen E, Boon T, Picard J.: "Cell- and stage-specific expression of Mage genes during mouse spermatogenesis". *Mammalian Genome*, 11, pp.696–699

De Backer *et al,* 1995 : De Backer O, Verheyden AM, Martin B, Godelaine D, De Plaen E, Brasseur R, Avner P, Boon T : « Structure, chromosomal location, and expression pattern of three mouse genes homologous to the human MAGE genes." Genomics 1995;28(1):74-83

Delmas *et al,* 2007: Delmas V, Beermann F, Martinozzi S, Carreira S, Ackermann J, Kumasaka M, Denat L, Goodall J, Luciani F, Viros A, Demirkan N, Bastian BC, Goding CR,Larue L.: "Beta-catenin induces immortalization of melanocytes by suppressing p16INK4a expression and cooperates with N-Ras in melanoma development." Genes Dev. 2007; 21(22):2923-35

De Plaen *et al,* 1994: De Plaen E, Arden K, Traversari C, Gaforio JJ, Szikora JP, De Smet C, Brasseur F, van der Bruggen P, Lethé B, Lurquin C, et al : « Structure, chromosomal localization, and expression of 12 genes of the MAGE family." Immunogenetics. 1994; 40 (5):360-9

De Smet *et al.*, 1995 : De Smet C, Courtois SJ, Faraoni I, Lurquin C, Szikora JP, De Backer O, Boon T. : « Involvement of two Ets binding sites in the transcriptional activation of the MAGE1 gene." Immunogenetics. 1995; 42(4):282-90

De Smet *et al,* 1996 : De Smet C, De Backer O, Faraoni I, Lurquin C, Brasseur F, Boon T.The activation of human gene MAGE-1 in tumor cells is correlated with genome-wide demethylation.. *Proc. Natl. Acad. Sci.*, 1996, pp.7149–7153

De Smet *et al*, 1999 : De Smet C, Lurquin C, Lethé B, Martelange V, Boon T.: "DNA Methylation Is the Primary Silencing Mechanism for a Set of Germ Line- and Tumor-Specific Genes with a CpG-Rich Promoter DNA Methylation Is the Primary Silencing Mechanism for a Set of Germ Line- and Tumor-Specific Genes with a CpG-Rich Promoter" *Molecular and Cellular Biology*, 1999 pp.7327–7335.

De Smet *et al*, 2004: Charles De Smet, Axelle Loriot, and Thierry Boon : « Promoter-Dependent Mechanism Leading to Selective Hypomethylation within the 5_ Region of Gene *MAGE-A1* in Tumor Cells » MOLECULAR AND CELLULAR BIOLOGY, 2004, p. 4781–4790

Dombret *et al*, 2012: Dombret C, Nguyen T, Schakman O, Michaud JL, Hardin-Pouzet H, Bertrand MJ, De Backer O. : « Loss of Maged1 results in obesity, deficits of social interactions, impaired sexual behavior and severe alteration of mature oxytocin production in the hypothalamus." Hum Mol Genet. 2012 ; 21(21):4703-17

Doyle *et al,* 2010 : Doyle JM, Gao J, Wang J, Yang M, Potts PR. : « MAGE-RING protein complexes comprise a family of E3 ubiquitin ligases » Mol Cell. 2010;39(6):963-74

Duan, Z. *et al*, 2003. Duan Z, Duan Y, Lamendola DE, Yusuf RZ, Naeem R, Penson RT, Seiden MV. : "Overexpression of MAGE / GAGE Genes in Paclitaxel / Doxorubicin-resistant Human Cancer Cell Lines." *Clinical Cancer Research*, 2003; pp.2778–2785

Ehrlich *et al*, 2002: Ehrlich, M., G. Jiang, E. Fiala, J. S. Dome, M. C. Yu, T. I. Long, B. Youn, O. S. Sohn, M. Widschwendter, G. E. Tomlinson, M. Chintagumpala, M. Champagne, D. Parham, G. Liang, K. Malik, and P. W. Laird: " Hypomethylation and hypermethylation of DNA in Wilms tumors." Oncogene 2002 21:6694–6702

Fearon, E.R. *et al.*, 1988: Fearon ER, Itaya T, Hunt B, Vogelstein B, Frost P.: "Induction in a Murine Tumor of Immunogenic Tumor Variants by Transfection with a Foreign Gene". *Cancer Research*, 1988; 48, pp.2975–2980

Forslund et Nordqvist, 2001: Ohman Forslund K, Nordqvist K.: "The melanoma antigen genes--any clues to their functions in normal tissues?" Exp Cell Res. 2001; 265(2):185-94

Gillespie & Coleman 1999: Gillespie, a M. & Coleman, R.E : « The potential of melanoma antigen expression in cancer therapy." *Cancer treatment reviews*, 1999 25(4), pp.219–227

Gillet et Gottesman, 2011: Jean-Pierre Gillet and Michael M. Gottesman : « Advances in the Molecular Detection of ABC Transporters Involved in Multidrug Resistance in Cancer" Curr Pharm Biotechnol. 2011; 12(4): 686–692

Gjerstorff *et al*, 2008 : Gjerstorff MF, Harkness L, Kassem M, Frandsen U, Nielsen O, Lutterodt M, Møllgård K, Ditzel HJ: "Distinct GAGE and MAGE-A expression during early human

development indicate specific roles in lineage differentiation." Hum Reprod. 2008;23(10):2194-201

Grem *et al*, 2011: Grem JL, Danenberg KD, Behan K, Parr A, Young L, Danenberg PV, Nguyen D, Drake J, Monks A, Allegra CJ.: " Dihydropyrimidine Dehydrogenase Profiles of Cell Lines of the National Cancer Institute ' s Anticancer Drug Screen Thymidine Kinase , Thymidylate Synthase , and Dihydropyrimidine Dehydrogenase Profiles of Cell Lines of the National Cancer Institute ' s An". *Clinical biochemistry*, 2011 pp.999–1009

Heisig, 2009:. Heisig p: "Type II topoisomerases--inhibitors, repair mechanisms and mutations." *Mutagenesis*, 2009 24(6), pp.465–9

Huijbers *et al*, 2006: Ivo J. Huijbers, Paul Krimpenfort, Patrick Chomez, Martin A. van der Valk, Ji-Ying Song, Else-Marit Inderberg-Suso, Anne-Marie Schmitt-Verhulst, Anton Berns, and Benoıˆt J. Van den Eynde: "An Inducible Mouse Model of Melanoma Expressing a Defined Tumor Antigen." Cancer Res 2006; 66: (6).

Jung *et al*, 2005: Jung, E.J. et al.: "Expression of family A melanoma antigen in human gastric carcinoma." *Anticancer research*, 2005; 25(3B), pp.2105–11.

Indra *et al*, 2007: Arup Kumar Indra, Eduardo Castaneda; Maria Cristina Antal, Ming Jiang, Nadia Messaddeq ,Xiangjun Meng, Christiane V. Loehr, Patricio Gariglio, Shigeaki Kato, Walter Wahli,Be´atrice Desvergne, Daniel Metzger and Pierre Chambon: "Malignant Transformation of DMBA/TPA-Induced Papillomas and Nevi in the Skin of Mice Selectively Lacking Retinoid-X-Receptor a in Epidermal Keratinocytes" Journal of Investigative Dermatology, 2007, 127

Krimpenfort *et al*, 2001: Krimpenfort, P., Quon, K.C., Mooi, W.J., Loonstra, A., and Berns, A.: "Loss of p16Ink4a confers susceptibility to metastatic melanoma in mice." *Nature 2001* 413: 83–86

Ladelfa *et al*, 2012 : Ladelfa MF, Peche LY, Toledo MF, Laiseca JE, Schneider C, Monte M.Cancer Lett. Tumor-specific MAGE proteins as regulators of p53 function. 2012 Dec 1;325(1):11-7. doi: 10.1016/j.canlet.2012.05.031

Laduron *et al*, 2004: Sandra Laduron, Rachel Deplus, Sifang Zhou, Olga Kholmanskikh, Danie`le Godelaine,Charles De Smet, S. Diane Hayward, Franc¸ois Fuks, Thierry Boon and Etienne De Plaen : « MAGE-A1 interacts with adaptor SKIP and thedeacetylase HDAC1 to repress transcription » Nucleic Acids Research, 2004, Vol. 32, No. 14 4340–4350

Liu *et al*, 2013: Wei Liu, Sonia Cheng, Sylvia L. Asa, and Shereen Ezzat: "The Melanoma-Associated Antigen A3 Mediates Fibronectin-Controlled Cancer Progression and Metastasis » Cancer Res 2008; 68:(19)

Loriot *et al*, 2006 : Axelle Loriot, Etienne De Plaen, Thierry Boon and Charles De Smet: "Transient Down-regulation of DNMT1 Methyltransferase Leads to Activation and Stable Hypomethylation of *MAGE-A1* in Melanoma Cells" *J. Biol. Chem. 2006*, 281:10118-10126

Loriot *et al*, 2012 : Loriot A, Parvizi GK, Reister S, De Smet C. : « Silencing of cancer germline genes in human preimplantation embryos: evidence for active de novo DNA methylation in stem cells.BiochemBiophys Res Commun. 2012; 417(1):187-91

Madisen et al, 2010: Linda Madisen, Theresa A Zwingman, Susan M Sunkin, Seung Wook Oh, Hatim A Zariwala, Hong Gu, Lydia L Ng, Richard D Palmiter, Michael J Hawrylycz, Allan R Jones, Ed S Lein & Hongkui Zeng: "A Robust and high-throughput Cre reporting and characterization system for the whole mouse brain"

Marcar *et al,* 2007 : Marcar L, Maclaine NJ, Hupp TR, Meek DW.: "Mage-A cancer/testis antigens inhibit p53 function by blocking its interaction with chromatin."Oncol Rep. 2007 18(2):329-36.

Marchand *et al,* 1995: Marchand M, Weynants P, Rankin E, Arienti F, Belli F, Parmiani G, Cascinelli N, Bourlond A, Vanwijck R, Humblet Y, et al.: "Tumor regression responses in melanoma patients treated with a peptide encoded by gene MAGE-3." Int J Cancer. 1995; 63(6):883-5

Meley *et al,* 2010: D Meley, DG Spiller, MRH White, H McDowell, B Pizer and V Se´e: "p53-mediated delayed NF-jB activity enhances etoposide-induced cell death in medulloblastoma" Cell Death and Disease, 2010 1, e41

Mhaidat *et al,* 2007 (a): Nizar M. Mhaidat, Yufang Wang, Kelly A. Kiejda, et al. : « Docetaxel-induced apoptosis in melanoma cells is dependent on activation of caspase-2" *Mol Cancer Ther* 2007;6:752-761

Mhaidat et al, 2007 (b): Nizar M. Mhaidat, Xu Dong Zhang, Chen Chen Jiang, et al. : « Docetaxel-Induced Apoptosis of Human Melanoma Is Mediated by Activation of c-Jun NH2-Terminal Kinase and Inhibited by the Mitogen-Activated Protein Kinase Extracellular Signal-Regulated Kinase 1/2 Pathway" *Clin Cancer Res* 2007;13:1308-1314

Monte *et al*, 2006: Monte M, Simonatto M, Peche LY, Bublik DR, Gobessi S, Pierotti MA, Rodolfo M, Schneider C. : « MAGE-A tumor antigens target p53 transactivation function through histone deacetylase recruitment and confer resistance to chemotherapeutic agents" Proc Natl Acad Sci U S A. 2006 J; 103(30):11160-5

Morishima *et al,* 2002: Morishima N, Nakanishi K, Takenouchi H, Shibata T and Yasuhiko Y: "An endoplasmic reticulum stress-specific caspase cascade in apoptosis. Cytochrome c-independent activation of caspase-9 by caspase-12." J Biol Chem 2002; 277: 34287-34294

Mouri *et al,* 2012: Akihiro Mouri, Aya Sasaki, Ken Watanabe, Chiharu Sogawa, Shigeo Kitayama, Takayoshi Mamiya, Yoshiaki Miyamoto, Kiyofumi Yamada, Yukihiro Noda and Toshitaka Nabeshima: "MAGE-D1 Regulates Expression of Depression-Like Behavior through Serotonin Transporter Ubiquitylation" J Neurosci. 2012; 32(13):4562-80

Muller *et al,* 2011: Patricia A. J. Muller, Karen H. Vousden, and Jim C. Norman: « p53 and its mutants in tumor cell migration and invasion" Journal of cell biology 2011;192(2):209-18

Nagao, T. *et al,* 2003: Nagao T, Higashitsuji H, Nonoguchi K, Sakurai T, Dawson S, Mayer RJ, Itoh K, Fujita J. : "MAGE-A4 interacts with the liver oncoprotein gankyrin and suppresses its tumorigenic activity." *The Journal of biological chemistry*, 2003; 278(12), pp.10668–74

Nguyen *et al,* 2010: Nguyen TH, Bertrand MJ, Sterpin C, Achouri Y, De Backer OR.: "Maged1, a new regulator of skeletal myogenic differentiation and muscle regeneration" BMC Cell Biol. 2010;11:57

Oakes *et al,* 2007 : Oakes CC, La Salle S, Smiraglia DJ, Robaire B, Trasler JM. : "Developmental acquisition of genome-wide DNA methylation occurs prior to meiosis in male germ cells." Dev Biol 2007a;307:368–379

Porporato *et al,* 2011: Porporato PE, Dhup S, Dadhich RK, Copetti T, Sonveaux P: "Anticancer targets in the glycolytic metabolism of tumors: a comprehensive review." Front Pharmacol. 2011; 2:49

Roger *et al,* 2006: Roger, L., Gadea, G. & Roux, P: "Control of cell migration: a tumour suppressor function for p53?" *Biology of the cell,* 2006 98(3), pp. 141–52

Sakurai *et al,* 2004 : Sakurai T, Itoh K, Higashitsuji H, Nagao T, Nonoguchi K, Chiba T, Fujita J : « A cleaved form of MAGE-A4 binds to Miz-1 and induces apoptosis in human cells." J Biol Chem. 2004; 279(15):15505-14

Sang *et al,* 2010: Sang M, Wang L, Ding C, Zhou X, Wang B, Wang L, Lian Y, Shan B. "Melanoma-associated antigen genes - an update.Cancer Letters" Cancer Lett. 2011; 302(2):85-90

Serrano *et al,* 1993: Serrano, M., Hannon, G.J., and Beach, D: "A new regulatory motif in cell-cycle control causing specific inhibition of cyclin D/CDK4". *Natur 1993* 366: 704–707

Serrano *et al,* 1996: Serrano, M., Lee, H., Chin, L., Cordon-Cardo, C., Beach, D., and DePinho, R.A: "Role of the INK4a locus in tumor suppression and cell mortality." *Cel, 1996* 85: 27–37

Soule *et al,* 2010: Soule HD, Maloney TM, Wolman SR, Peterson WD Jr, Brenz R, McGrath CM, Russo J, Pauley RJ, Jones RF, Brooks SC.: "Isolation and characterization of a spontaneously immortalized human breast epithelial cell line, MCF-10." Cancer Res. 2010; 70(24):10362-70

Sun *et al,* 2007: Xiao-Xin Sun, Mu-Shui Dai and Hua Lu: "5-Fluorouracil Activation of p53 Involves an MDM2-Ribosomal Protein Interaction" *J. Biol. Chem. 2007, 282:8052-8059*

Suzuki *et al,* 2007: Suzuki T, Yoshida K, Wada Y, Hamai Y, Sentani K, Oue N, Yasui W: "Melanoma-associated antigen-A1 expression predicts resistance to docetaxel and paclitaxel in advanced and recurrent gastric cancer" Oncol Rep. 2007; 18(2):329-36

Takahashi, K. *et al.,* 1995. Takahashi K, Shichijo S, Noguchi M, Hirohata M, Itoh K : « Identification of MAGE-1 and MAGE-4 Proteins in Spermatogonia and Primary Spermatocytes of Testis Advances in Brief Identification of MAGE-1 and MAGE-4 Proteins in Spermatogonia and Primary Spermatocytes of Testis" *Cancer Research*, 1995; 55, pp.3478–3482

Thottassery *et al,* 1997: JAIDEEP V. THOTTASSERY, GERARD P. ZAMBETTI, KAZUHIKO ARIMORI, ERIN G. SCHUETZ, AND JOHN D. SCHUETZ: "p53-dependent regulation of *MDR1* gene expression causes selective resistance to chemotherapeutic agents" *Proc. Natl. Acad. Sci. USA, 1997* Vol. 94, pp. 11037–11042

Traversari *et al,* 1992 : Traversari C, van der Bruggen P, Luescher IF, Lurquin C, Chomez P, Van Pel A, De Plaen E, Amar-Costesec A, Boon T. : « A nonapeptide encoded by human gene MAGE-1 is recognized on HLA-A1 by cytolytic T lymphocytes directed against tumor antigen MZ2-E." J Exp Med. 1992; 176(5):1453-7

Tsao *et al*, 1998: Tsao, H., Benoit, E., Sober, A.J., Thiele, C., and Haluska, F.G: "Novel mutations in the p16/CDKN2A binding region of the cyclin-dependent kinase-4 gene" *Cancer Res* 1998. 58: 109–113

van der Bruggen *et al*, 1991 :van der Bruggen P, Traversari C, Chomez P, Lurquin C, De Plaen E, Van den Eynde B, Knuth A, Boon T. : « A gene encoding an antigen recognized by cytolytic T lymphocytes on a human melanoma" Science. 1991; 254(5038):1643-7

van Pel, *et al*, 1992 : van Pel, A., Vessière, F. & Boon, T: "Protection against two spontaneous mouse leukemias conferred by immunogenic variants obtained by mutagenesis" *J. Exp. Med.*, 1983 157, pp.1992–2001

van Roy & Berx, 2008: van Roy, F. & Berx, G: "Review The cell-cell adhesion molecule E-cadherin" *Cellular and Molecular Life Sciences*, 2008; 65, pp.3756–3788

Wang, X. *et al.*, 2010: Wang X, Tang J, Xing L, Shi G, Ruan H, Gu X, Liu Z, Wu X, Gao X, Xu Y.: "Interaction of MAGED1 with nuclear receptors affects circadian clock function" *The EMBO journal*, 2010; 29(8), pp.1389–400

Weber *et al.*, 1994: Weber J, Salgaller M, Samid D, Johnson B, Herlyn M, Lassam N, Treisman J, Rosenberg SA.: "Expression of the MAGE-1 tumor antigen is up-regulated by the demethylating agent 5-aza-2'-deoxycytidine." Cancer Res. 1994; 54(7):1766-71

Wischnewski *et al.*, 2006: Wischnewski F, Pantel K, Schwarzenbach H.: "Promoter demethylation and histone acetylation mediate gene expression of MAGE-A1, -A2, -A3, and -A12 in human cancer cells." Mol Cancer Res. 2006; 4(5):339-49

Yang *et al*, 2007: Yang B, O'Herrin SM, Wu J, Reagan-Shaw S, Ma Y, Bhat KM, Gravekamp C, Setaluri V, Peters N, Hoffmann FM, Peng H, Ivanov AV, Simpson AJ, Longley BJ: "MAGE-A, mMage-b, and MAGE-C proteins form complexes with KAP1 and suppress p53-dependent apoptosis in MAGE-positive cell lines" Cancer Res. 2007; 67 20: 9954-62

Yuspa et al, 1998: Yuspa SH: "The pathogenesis of squamous cell cancer: lessons learned from studies of skin carcinogenesis" J Dermatol Sci, 1998; 17:1–7 1260

Zhao *et al*, 2006 : Ying Zhao, Shaoli Lu, Lipeng Wu, Guolin Chai, Haiying Wang, Yingqi Chen, Jia Sun, Yu Yu, Wen Zhou, Quanhui Zheng, Mian Wu, Gregory A. Otterson and Wei-Guo Zhu: "Acetylation of p53 at Lysine 373/382 by the Histone Deacetylase Inhibitor Depsipeptide Induces Expression of $p21^{Waf1/Cip}$ Mol. Cel Biol 2006 vol 26 no. 7 2782-2790

ABREVIATIONS

5-FU	5-fluorouracile
ABC	ATP-binding cassette
APC	Antigen-Presenting Cell
ARF	Alternate open Reading Frame
ATM	Ataxia Telangiectasia Mutated
BAC	Bacterial Artificial Chromosome
Bax	Bcl-2-Associated X protein
Bcl-2	B-Cell Lymphoma 2
Bcl-xL	B-Cell Lymphoma-extra large
BSA	Bovine Serum Albumin
CDK	Cycline Dependent Kinase
CDKN2A	Cyclin Dependent Kinase Inhibitor 2A
cDNA	Complementary DeoxyriboNucleic Acid
CT	Control
CTA	Cancer Testis Antigen
DMBA	Dimethylbenz(a)anthracene
DMEM	Dulbeco's Modified Eagle Medium
DMSO	DiMethylSulfOxyde
DNA	DeoxyriboNucleic Acid
DNMT	DNA methytransferase
EDTA	Ethylenediaminetetraacetic acid
FACS	Fluorescent-Activated Cell Sorting
FBS	Fetal Bovine Serum
FGF	Fibroblast Growth Factor
GAGE	G Antigen
GAPDH	GlycerAldehydes-3-Phosphate
HBS	Hepes Buffered Saline
HDAC	Histone Deacetylase
hEGF	Human Epithelial Growth Factor
HIF-1	Hypoxia Inductible Factor 1
HLA	Human Leucocyte Antigens
HRP	HorseRadish Peroxydase
HS	Horse Serum
IC50	Half Maximal Inhibitory Concentration
INK4	Inhibitor of Cyclin-Dependent Kinase 4
KAP-1	Krüppel Associated protein-1
KU-80	Lupus Ku Autoantigen Protein p80
MAGE	Melanoma Antigen
MDM2	Mouse Double Minute 2

MHC	Major Histocompatibility Complex
MHD	Mage Homology Domain
Miz-1	Myc-interacting zinc finger protein 1
MTT	3-(4,5-dimethylthiazol-yl)-2,5-diphenyltetrazolium bromide
NT	No Treatment
PAGE	Polyacrylamide Gel Electrophoresis
PBS	Phosphate Buffer Saline
PCR	Polymerase Chain Reaction
PGK	PhosphoGlycerate Kinase
PHD2	Prolyl-Hydroxylase 2
PS	Penicilin/Streptomycin
Puma	p53 Upregulated Modulator of Apoptosis
PVDF	PolyVinylineDiFluoride
Ras	Rat Sarcoma oncogene
Rb	Retinoblastoma
RING	Really Interesting New Gene
RNA	RiboNucleic Acid
SAP	Shrimp Alkaline Phosphatase
SDS	Sodium Dodecyl Sulfate
SKIP	Ski interacting protein
TET	TET methylcytosine dioxygenase 1
TPA	12-O-tetradecanoylphorbol-13acetate
TRIM28	Tripartite motif-containing 28
TyrP	Tyrosinase Promoter
UV	UltraViolet
VHL	Von Hippel Lindau
WT	Wild-type
XAGE	X Chromosome Antigen
YAC	Yeast Artificial Chromosome